

MSc Mathematics

Track: Bio-math

Master thesis

Semi-discrete modelling in population dynamics, including stage structure and birth potential

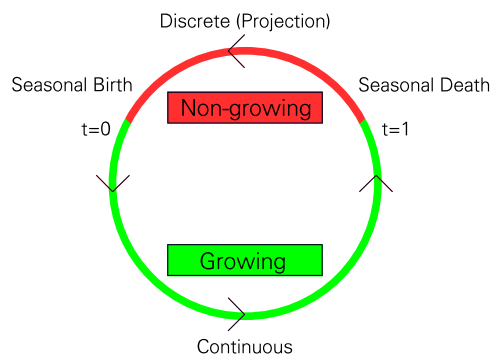
by

Jaap Schouten

March 19, 2018

Supervisor: dr. A.J. (Ale Jan) Homburg

Second examiner: dr. Bob Planqué



Department of Mathematics
Faculty of Sciences



Abstract

We consider a semi-discrete population dynamics model with a mechanistic justification where we distinguish a growing season and a non-growing season. The resource-consumer interaction studied includes a stage-structure and seasonal birth governed by a birth potential. The species considered is iteroparous and maturation and birth are modelled as discrete events. We derive a discrete year to year consumer map modelling the evolution of the consumer species. This map may lead to extinction, a stable steady state or population cycles through a transcritical and a Neimark-Sacker bifurcation respectively. We prove existence of the non-trivial steady state and determine a domain for the steady state solution. We also show how Arnold tongues can produce not only dense orbits on an invariant curve but also stable periodic behaviour. In addition we extend the model to include delayed reproduction and a niche shift in feeding after maturation. These models may be useful in explaining the dynamics produced by larger mammals.

Keywords: *Population dynamics; Stage-structure; Birth potential; Consumer-resource; Semi-discrete modelling; Iteroparous; Neimark-Sacker bifurcation; Arnold tongues; Population cycles*

Title: Semi-discrete modelling in population dynamics, including stage structure and birth potential

Author: Jaap Schouten, j2.schouten@student.vu.nl, 2503230

Supervisor: dr. A.J. (Ale Jan) Homburg

Second examiner: dr. Bob Planqué

Date: March 19, 2018

Department of Mathematics
VU University Amsterdam
de Boelelaan 1081, 1081 HV Amsterdam
<http://www.math.vu.nl/>

Contents

| | | |
|---------------------|--|-----------|
| 1 | Popular summary | 4 |
| 2 | Introduction | 5 |
| 3 | Theory | 9 |
| 3.1 | Model Formulation | 9 |
| 3.1.1 | Chemostatic resource dynamics | 10 |
| 3.1.2 | Logistic resource dynamics | 11 |
| 3.2 | Rescaling | 12 |
| 3.3 | Time scale separation | 13 |
| 3.3.1 | Chemostatic resource dynamics | 13 |
| 3.3.2 | Logistic resource dynamics | 14 |
| 4 | Results | 15 |
| 4.1 | Logistic resource with discrete death | 15 |
| 4.1.1 | Solving the continuous growing season dynamics | 15 |
| 4.1.2 | Stability analysis | 17 |
| 4.2 | Logistic resource with continuous death | 30 |
| 4.2.1 | Solving the continuous growing season dynamics | 30 |
| 4.2.2 | Stability analysis | 33 |
| 4.3 | Generalisation to multiple stage model | 36 |
| 4.3.1 | Dynamics of the two year maturation model | 38 |
| 4.3.2 | n -year maturation model | 40 |
| 4.4 | Starvation | 40 |
| 4.5 | Chemostatic resource growth | 41 |
| 4.6 | Niche Shift | 42 |
| 5 | Conclusion | 45 |
| Bibliography | | 47 |

1 Popular summary

When developing mathematical models of ecological systems it is difficult to look beyond the influence of the seasons on nature. Behaviour and abundance of species and resources may be vastly different during different periods of the year, especially in places far away from the equator. Therefore, this has a great influence on the dynamics and growth of animals. In this thesis a model is presented which includes the difference between a growing season (spring and summer) and a non-growing season (fall and winter). To model these different dynamics we use both continuous modelling techniques for processes which are more gradual such as species growth, and discrete modelling techniques for events which are restricted to a short period of the year such as giving birth.

We formulate a model in which the interaction between a consumer species and resource is studied. We focus on how this consumer can be split into a juvenile and adult population, where the adults produce the biomass of the offspring for the next year during the growing season (such as eggs). These dynamics can be solved analytically when assuming the resource grows much quicker than the consumer does. From this we are able to derive a discrete system describing the evolution of the consumer species biomass.

To assess the behaviour of the resulting discrete system we must analyse the possible steady states and their stability. We use analytic and numerical tools to understand the different behaviours that can be found. This shows how the species can go extinct, have a stable non-negative steady state or can generate more complex behaviour such as population cycles and periodic orbits. Initially we focus on a model in which the juveniles mature after a single year and extend this to a model where maturation takes several years such as is more likely in larger mammals.

2 Introduction

In population dynamics the goal is to study the mechanisms of growth and interaction of species. This can help to understand the regulation of populations of species and give insight into how complex dynamics are generated. The abstraction of the real-world dynamics into a rigorous mathematical model can be used as a tool to better comprehend and potentially influence the ecology of the world around us.

In nature periodic behaviour is commonplace. Therefore, cyclic behaviour can be found throughout mathematical models of biological phenomena. However, how to include seasonal behaviour into a mathematical model can present many challenges. In this thesis a model setting will be presented in which seasonal behaviour in population dynamics can be accounted for. This allows for the distinction in a year between a growing season and a non-growing season as is found in many ecological systems.

The seasons provide a guideline for nature along which the yearly life cycle unfolds. For many species breeding is a discrete event in which during a short period of the year (or possibly a different cycle) new juveniles are born. This mostly happens during the spring, after which the species can grow optimally during the following seasons. This seasonal behaviour is an essential part of many species and life as we know it. Therefore, we want to find a way of accounting for these different stages of a year.

Historic context Already a large amount of models accounting for this discrete behaviour have been developed. For example, the Ricker model [1] and the Beverton-Holt model [2] are examples of single species discrete time models which have provided ways to interpret certain species dynamics through relatively simple models. These works have found applications in the modelling of fisheries but have later also been derived in different contexts. Their dynamics are given by

$$\text{Ricker model: } N_{t+1} = N_t e^{r(1 + \frac{N_t}{K})}, \quad (2.1)$$

$$\text{Beverton-Holt model: } N_{t+1} = \frac{R_0 N_t}{1 + \frac{N_t}{M}}. \quad (2.2)$$

Discrete modelling can also be used when including consumer-resource or parasitoid-host interactions, as for instance is done by Nicholson-Bailey [3]. They examined

the relation between a parasitoid which lays its eggs inside another animal which is called the host, as is done by some insects. An overview of such discrete time models can be found in Murdoch [4]. The dynamics of the Nicholson-Bailey model for a host H and parasitoid P including density dependence are given by

$$H_{t+1} = H_t e^{r(1 - \frac{H_t}{K})} e^{-aP_t}, \quad (2.3)$$

$$P_{t+1} = cH_t (1 - e^{-aP_t}). \quad (2.4)$$

Stage-Structure When we consider the inclusion of (seasonal) breeding into a model, it is also reasonable to think of differentiating the species into different developmental stages. We may consider the splitting into a juvenile stage and an adult stage where the juveniles are the newborn population that do not yet reproduce and the adults that are reproducing. Such splitting is called a stage-structure. Alternatively a splitting into age groups can also be made.

Discrete matrix models embodying such a structure were developed independently in the 1940s by Bernardelli [5], Lewis [6] and Leslie [7]. The Leslie matrix is an example which describes the growth of a population which exhibits periodic breeding and can be used to derive the resulting age distribution. Such models do not include different seasons or interactions with a resource.

Structured semi-discrete models To be able to represent the changes in different seasons we propose the setting of splitting a year into two periods that each will be modelled differently. On the one hand we model the growing season as a continuous system, on the other hand the non-growing season will be represented by a discrete event in which seasonal reproduction and possibly a winter survival probability is included. This method is visualised in Figure 2.1. This is in contrast to existing matrix models where all seasons were modelled as a discrete process (Caswell and Trevisan [8], Katsanevakis and Verriopoulos [9], Mc Fadden [10]).

Techniques where structured populations are combined with semi-discrete modelling were introduced in de Roos [11]. Expanding on this models studying consumer-resource interaction in growth and maturation of juveniles of stage-structured populations have been developed (de Roos et al. [12], [13]; Guill [14]; Wollrab [15]). In addition Gyllenberg [16] and Gamarra [17] showed how complex behaviour such as cycles or chaotic behaviour can arise from modelling stage-structured or competing species.

Similar models have also been developed to study unstructured species, where only a resource, an adult population and a birth potential is considered. For example Geritz & Kisdi [18] studied a single stage species model in which at the end of each year the current adult population dies and through a time-scale

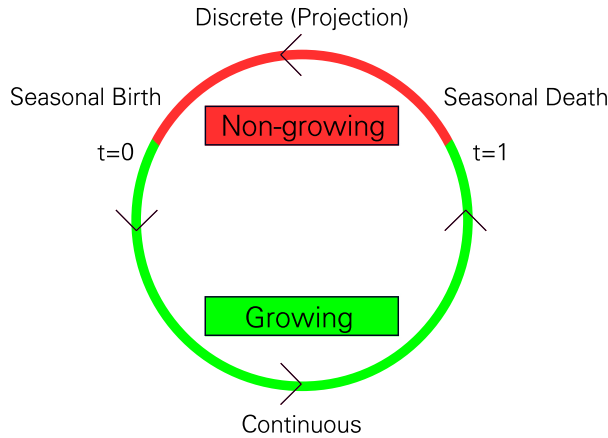


Figure 2.1: An illustration of the two stage seasonal model, in which the green part of the year represents the growing season and the red part represents the non-growing season.

argument they derived various analytical results for this model. Additions to this have been made for example including cannibalism as presented by Eskola [19].

Research questions The setting we would like to consider is that of a stage-structured semi-discrete model of a resource interacting with a population of juveniles and adults where breeding is governed using a birth-potential. The consumer is assumed to be iteroparous, meaning they can reproduce multiple times. This context was also considered by Sun [20] where a numerical investigation is made for a model containing multiple resources (niche shift) and a continuous transition from juvenile to adult. This provides an explanation for the observation of alternative stable states.

The same modelling setting can also be used to study patterns in a patched population model [21], where the dynamics of species at different interacting locations was studied. In this they also derived a second-order map for an isolated population in the case of no interaction between resource and juveniles and noted that if it were present it could result in population cycles. However, no further analysis of this situation was given. In Davydova et al. [22] a detailed analysis for a semelparous population without a resource interaction is given.

Combining stage-structure and seasonality presents the challenge of combining them in such a way to allow for a broad interpretation yet provide as much mathematical insights as possible. We will show how using two-time scale analysis a discrete two-dimensional map can be derived belonging to a stage-structured population and show how it can exhibit different dynamics.

In addition we will consider the difference between species with non-overlapping generations, meaning after each year all juveniles will become adults which is applicable to many smaller animals such as insects, and overlapping generations where it takes multiple years to reach adulthood which is more common for vertebrates. At first we will study a model for non-overlapping generations which provides more detailed analytical results and extend this to the case of overlapping generations.

3 Theory

The model we will study will be a biomass model including stage-structure. This means we will split the total population in a juvenile (non reproducing) and adult (reproducing) population. A derivation of such a model can be found in de Roos et al. [13], where it is derived from a fully physiologically structured population. We will simplify this model by having a seasonal instead of continuous transition from juvenile to adult while excluding the option of starvation. Examples of such models, however without the stage-structure, can be found in Geritz & Kisdi [18].

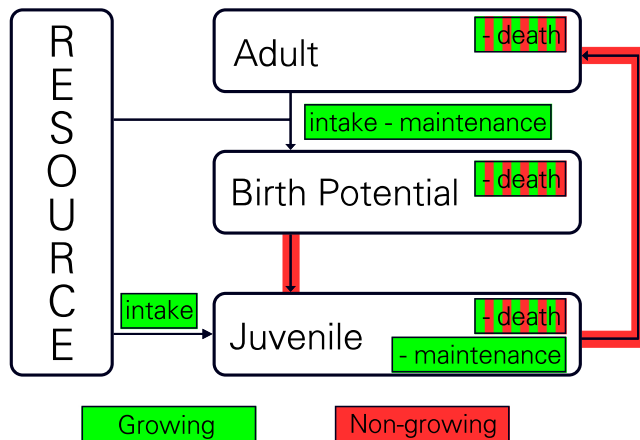


Figure 3.1: Outline of the relations between the different variables in the system.

3.1 Model Formulation

In the most general setting we are going to consider a dynamical system consisting of a continuous phase, which will describe the dynamics during a season, and a discrete phase or projection, which will describe the between season dynamics. Through this projection the new initial values of the continuous phase for the next season are obtained.

We will first describe a system consisting of four variables. The species we are investigating is split into a juvenile group J and an adult group A . Here we

assume, for the sake of simplicity, that juveniles reach sexual maturity after a single season. In further generalisations a longer duration for maturation can be considered. Thus for now, after each season the juveniles of that season will be added to the adults. Both the juveniles and adults will be feeding from a single resource R . Reproduction shall occur through a birth potential B . This variable will accumulate biomass (eg. eggs or a growing foetus) during the season which shall be born or hatch at the beginning of the next season. To indicate which season the variable belongs to we will write J_n , A_n , R_n and B_n where $n \in \mathbb{N}$ indicates the season.

This continuous system shall be described by

$$C : \mathbb{R}^4 \rightarrow \mathbb{R}^4 \quad \text{with} \quad \begin{pmatrix} R_n(0) \\ J_n(0) \\ A_n(0) \\ B_n(0) \end{pmatrix} \mapsto \begin{pmatrix} R_n(T) \\ J_n(T) \\ A_n(T) \\ B_n(T) \end{pmatrix}. \quad (3.1)$$

Where T indicates the length of the season and the functions $R_n(t)$, $J_n(t)$, $A_n(t)$ and $B_n(t)$ are the solutions to a, later to be described, set of differential equations. After each season we will make a projection from the final state of season n to the initial state of season $n + 1$, as in

$$P : \mathbb{R}^4 \rightarrow \mathbb{R}^4 \quad \text{with} \quad \begin{pmatrix} R_n(T) \\ J_n(T) \\ A_n(T) \\ B_n(T) \end{pmatrix} \mapsto \begin{pmatrix} R_n(T) \\ B_n(T) \\ A_n(T) + J_n(T) \\ 0 \end{pmatrix}. \quad (3.2)$$

The composition of C and P give the dynamics from season to season. Thus we define

$$S : \mathbb{R}^4 \rightarrow \mathbb{R}^4 \quad \text{with} \quad S = P \circ C. \quad (3.3)$$

3.1.1 Chemostatic resource dynamics

The first model we will consider is one based on a resource which, without any consumer present, behaves as in a chemostat. Thus we would have $\dot{R} = \rho(R_m - R)$, where R_m is the influx and efflux concentration of the resource into the system and ρ the influx rate into the system. When we add a consumer which feeds on the resource at intake rate I_m for the juveniles and θI_m for the adults (and thus θ gives the ratio between the feeding rate of juvenile and adult) we obtain the differential equation

$$\dot{R}_n = \rho(R_m - R_n) - I_m R_n J_n - \theta I_m R_n A_n.$$

Such dynamics can be considered when the consumer is for example a fish population in a lake that has a influx and efflux of resource while the fish stay in the lake. Thus the consumer species will not have a dilution term.

Now for the dynamics of the juveniles we have an increase in biomass due to feeding on the resource. This resource is being converted at an efficiency σ . We also consider an amount of the resource being needed for maintenance instead of growth which is accounted for by a rate q . The juvenile population has a death rate μ_c . This gives the differential equation for the juveniles as in

$$\dot{J}_n = \sigma I_m R_n J_n - q J_n - \mu_c J_n.$$

The within-season dynamics of the adult population is quite simple, since it only consists of a death rate. This is equal to the death rate of the juveniles, being μ_c . We assume that the adults invest all biomass in creation of birth-potential and not in growth. Thus the differential equation is

$$\dot{A}_n = -\mu_c A_n.$$

For the birth-potential, the dynamics are dependent on the size of the adult population and the energy/biomass that the adults have from consuming the resource. We assume that, similarly to the juveniles, the adults have an efficiency in converting the resource of σ . The birth-potential also declines with death-rate μ_c . For the maintenance rate q we assume it scales similarly to the intake rate with a factor θ . Thus we have the differential equation

$$\dot{B}_n = \sigma \theta I_m R_n A_n - q \theta A_n - \mu_c B_n.$$

It is important to note that, in this, we assume that during the season there does not occur any starvation, such that $\sigma I_m R_n - q$ remains positive. If not we would have to add starvation to the adult population as well when the quantity becomes negative [20].

We have derived the full set of differential equation to which C must adhere in case of a chemostatic resource, being

$$C_{\text{chem}} : \begin{cases} \dot{R}_n = \rho(R_m - R_n) - I_m R_n J_n - \theta I_m R_n A_n, \\ \dot{J}_n = \sigma I_m R_n J_n - q J_n - \mu_c J_n, \\ \dot{A}_n = -\mu_c A_n, \\ \dot{B}_n = \sigma \theta I_m R_n A_n - q \theta A_n - \mu_c B_n. \end{cases} \quad (3.4)$$

3.1.2 Logistic resource dynamics

An alternative model we will consider is a model where the resource exhibits logistic growth in absence of any consumers. Thus its dynamics would be described by

the continuous logistic equation $\dot{R} = \rho R(R_m - R)$, where R_m is the carrying capacity and ρR_m is the intrinsic growth rate of the population. Thus the system of differential equations becomes

$$C_{\log} : \begin{cases} \dot{R}_n = \rho R_n(R_m - R_n) - I_m R_n J_n - \theta I_m R_n A_n, \\ \dot{J}_n = \sigma I_m R_n J_n - q J_n - \mu_c J_n, \\ \dot{A}_n = -\mu_c A_n, \\ \dot{B}_n = \sigma \theta I_m R_n A_n - q \theta A_n - \mu_c B_n. \end{cases} \quad (3.5)$$

In addition we will also consider a model where the death rate during the season is zero, but where we add it into the between season dynamics. This would represent a system where mortality during the growing season is zero but the mortality in the non-growing season is much higher, as in a difference between summer and winter with low predation during the season. The continuous system then simplifies to

$$C_{\log; \mu_c=0} : \begin{cases} \dot{R}_n = \rho R_n(R_m - R_n) - I_m R_n J_n - \theta I_m R_n A_n, \\ \dot{J}_n = \sigma I_m R_n J_n - q J_n, \\ \dot{A}_n = 0, \\ \dot{B}_n = \sigma \theta I_m R_n A_n - q \theta A_n. \end{cases} \quad (3.6)$$

The projection then gains the survival probability μ_d which represents the probability of surviving the non-growing season. Thus it becomes

$$P_{\mu_d} : \mathbb{R}^4 \rightarrow \mathbb{R}^4 \quad \text{with} \quad \begin{pmatrix} R_n(T) \\ J_n(T) \\ A_n(T) \\ B_n(T) \end{pmatrix} \mapsto \begin{pmatrix} R_n(T) \\ \mu_d B_n(T) \\ \mu_d A_n(T) + \mu_d J_n(T) \\ 0 \end{pmatrix}. \quad (3.7)$$

3.2 Rescaling

Before we make any analysis of the systems we will rescale the variables. First of all we will scale the time using $\tau := t/T$ such that the continuous system will be on the domain $[0, 1]$. This also means we scale all rates (ρ, I_m, q, μ_c) with a factor T . However for the sake of simplicity we will not rename these.

We will also rescale the different variables using $r := R/R_m$, $j = I_m J$, $a = I_m \theta A$ and $b = I_m \theta B$. We also define the new parameter $\delta := \sigma I_m R_m$. This parameter can be seen as the adaptedness of the species to the environment (read resource), since when either the efficiency of the resource conversion, the intake rate or the amount of resource increases the fitness of the species increases.

This gives the rescaled systems, for the chemostatic model

$$C_{\text{chem}} : \begin{cases} \frac{\partial r}{\partial \tau} = \rho(1 - r) - rj - ra, \\ \frac{\partial j}{\partial \tau} = \delta rj - qj - \mu_c j, \\ \frac{\partial a}{\partial \tau} = -\mu_c a, \\ \frac{\partial b}{\partial \tau} = \delta \theta r a - q \theta a - \mu_c b, \end{cases} \quad (3.8)$$

for the logistic model with continuous death

$$C_{\log} : \begin{cases} \frac{\partial r}{\partial \tau} = \rho r(1 - r) - rj - ra, \\ \frac{\partial j}{\partial \tau} = \delta rj - qj - \mu_c j, \\ \frac{\partial a}{\partial \tau} = -\mu_c a, \\ \frac{\partial b}{\partial \tau} = \delta \theta r a - q \theta a - \mu_c b, \end{cases} \quad (3.9)$$

and for the logistic model with seasonal death

$$C_{\log; \mu_c=0} : \begin{cases} \frac{\partial r}{\partial \tau} = \rho r(1 - r) - rj - ra, \\ \frac{\partial j}{\partial \tau} = \delta rj - qj, \\ \frac{\partial a}{\partial \tau} = 0, \\ \frac{\partial b}{\partial \tau} = \delta \theta r a - q \theta a. \end{cases} \quad (3.10)$$

The projection for the non-growing season now becomes

$$P_{\mu_d} : \mathbb{R}^4 \rightarrow \mathbb{R}^4 \quad \text{with} \quad \begin{pmatrix} r_n(1) \\ j_n(1) \\ a_n(1) \\ b_n(1) \end{pmatrix} \mapsto \begin{pmatrix} r_n(1) \\ \frac{\mu_d}{\theta} b_n(1) \\ \mu_d a_n(1) + \mu_d \theta j_n(1) \\ 0 \end{pmatrix}. \quad (3.11)$$

3.3 Time scale separation

We can simplify the systems described by assuming that the continuous dynamics of the resource are much faster than the continuous dynamics of the other variables. This means the resource will assume an equilibrium on the fast time scale ($t = T\tau$) which decouples this equation from the rest.

3.3.1 Chemostatic resource dynamics

To get a separation of time scales we will assume that $0 < \delta, q, \mu_c \ll \rho, 1$ such that $\frac{\delta}{T} \approx \frac{q}{T} \approx \frac{\mu_c}{T} \approx 0$. This leads to a system for the ‘fast’ dynamics being

$$\text{Fast Dynamics: } \begin{cases} T \frac{\partial r}{\partial t} = \rho(1 - r) - rj - ra, \\ \frac{\partial j}{\partial t} = \frac{\partial a}{\partial t} = \frac{\partial b}{\partial t} = 0. \end{cases} \quad (3.12)$$

And the corresponding system for the slow dynamics

$$\text{Slow Dynamics: } \begin{cases} \frac{\partial j}{\partial \tau} = \delta \bar{r}(a, j)j - qj - \mu_c j, \\ \frac{\partial a}{\partial \tau} = -\mu_c a, \\ \frac{\partial b}{\partial \tau} = \delta \theta \bar{r}(a, j)a - q\theta a - \mu_c b, \end{cases} \quad (3.13)$$

where $\bar{r}(a, j) = \frac{\rho}{\rho + j + a}$ is the quasi-equilibrium of the fast system. This state is asymptotically stable since $\frac{\partial}{\partial r}(T \frac{\partial r}{\partial t}) = -(\rho + j + a) < 0$ for positive values of j and a .

3.3.2 Logistic resource dynamics

Similarly to the chemostatic case we can make a two time scale analysis for the logistic resource dynamics by assuming $0 < \delta, q, \mu_c \ll \rho, 1$. The ‘fast’ dynamics we now obtain are

$$\text{Fast Dynamics: } \begin{cases} T \frac{\partial r}{\partial t} = \rho r(1 - r) - rj - ra, \\ \frac{\partial j}{\partial t} = \frac{\partial a}{\partial t} = \frac{\partial b}{\partial t} = 0, \end{cases} \quad (3.14)$$

which looks very similar to (3.12). However, this system gives for the quasi-equilibrium $\bar{r}(a, j) = 1 - \frac{j+a}{\rho}$. With the corresponding slow dynamics

$$\text{Slow Dynamics: } \begin{cases} \frac{\partial j}{\partial \tau} = \delta \bar{r}(a, j)j - qj - \mu_c j, \\ \frac{\partial a}{\partial \tau} = -\mu_c a, \\ \frac{\partial b}{\partial \tau} = \delta \theta \bar{r}(a, j)a - q\theta a - \mu_c b. \end{cases} \quad (3.15)$$

We will later on see how this system is more suited to analytic solutions than the chemostatic system.

To asses the stability of \bar{r} we observe

$$\frac{\partial}{\partial r}(T \frac{\partial r}{\partial t}) = \rho - j - a - 2\rho \bar{r} = -\rho \bar{r}$$

which is negative for $\bar{r} > 0$. Thus in this case the equilibrium is asymptotically stable. This occurs for high enough growth rate of the resource to sustain the population of juveniles and adults since $\bar{r}(a, j) = 1 - \frac{j+a}{\rho}$ is positive for $\rho > j + a$. Note here that we rescaled the original ρ to $\rho R_m T$.

The time scale separation for the seasonal death model goes similarly with $\mu_c = 0$. It will result in the same $\bar{r}(j, a)$, with the slightly adjusted slow dynamics

$$\text{Slow Dynamics: } \begin{cases} \frac{\partial j}{\partial \tau} = \delta \bar{r}(a, j)j - qj, \\ \frac{\partial a}{\partial \tau} = 0, \\ \frac{\partial b}{\partial \tau} = \delta \theta \bar{r}(a, j)a - q\theta a. \end{cases} \quad (3.16)$$

4 Results

4.1 Logistic resource with discrete death

In this section we will discuss the model where resource dynamics is governed logically and the death process is only modelled during the non-growing season. We saw that in this case the resource will go to a (stable when $j + a < \rho$) quasi-steady state of $\bar{r}(a, j) = 1 - \frac{j+a}{\rho}$. The continuous dynamics of the adult population also simplifies to $\frac{\partial a}{\partial \tau} = 0$, thus $a(t) = a(0) = a_0$. Using these two results we obtain the two differential equations

$$\frac{\partial j(\tau)}{\partial \tau} = -\frac{\delta}{\rho} j(\tau)^2 + \left(\delta - \frac{\delta}{\rho} a_0 - q \right) j(\tau), \quad (4.1)$$

for the juvenile population and

$$\frac{\partial b(\tau)}{\partial \tau} = \delta \theta \left(1 - \frac{j(\tau) + a_0}{\rho} \right) a_0 - q \theta a_0, \quad (4.2)$$

for the birth potential.

4.1.1 Solving the continuous growing season dynamics

Solution for the end of growing season juvenile state In the equation for the juvenile population (4.1) we recognise the logistic differential equation as we have $\frac{\partial j(\tau)}{\partial \tau} = \alpha j(\tau) (\frac{\beta}{\alpha} - j(\tau))$, in which $\alpha = \frac{\delta}{\rho}$ and $\beta = \delta - \frac{\delta}{\rho} a_0 - q$. Here $\frac{\beta}{\alpha}$ is the carrying capacity of the system and β is the intrinsic growth rate associated with the system. Note that this can become negative when δ (the adaptedness to the environment) is too low. We will assume that at least $\delta > q$ such that there are values of a_0 such that the juvenile population grows during the season.

For the solution of (4.1) we have

$$j(\tau) = \frac{\beta c e^{\beta \tau}}{\alpha c e^{\beta \tau} + 1}, \quad \text{for some constant } c \in \mathbb{R},$$

which is a simplification of the result we obtain in (4.18). Now using $j(0) = j_0$ we obtain $c = \frac{j_0}{\beta - \alpha j_0}$ and thus can rewrite

$$j(\tau) = \frac{\beta j_0 e^{\beta \tau}}{\alpha j_0 e^{\beta \tau} + \beta - \alpha j_0}. \quad (4.3)$$

And we obtain that the end of season state for the juveniles is given by

$$j(1) = \frac{\beta(a_0)j_0e^{\beta(a_0)}}{\alpha j_0e^{\beta(a_0)} + \beta(a_0) - \alpha j_0}.$$

We write $\beta(a_0)$ to stress that this parameter is dependent on the seasons initial condition for the adult population.

Solution for the end of growing season birth potential Observe that now we have found the solution for $j(\tau)$ we can simply integrate (4.2) to obtain the solution for the birth potential. This gives, using that the birth potential at the beginning of the season is zero ($b(0) = 0$),

$$b(\tau) = \int_0^\tau \frac{\partial b(t)}{\partial t} dt = \left(\delta\theta a_0 - q\theta a_0 - \frac{\delta\theta}{\rho} a_0^2 \right) t - \frac{\delta\theta a_0}{\rho} \int_0^\tau j(t) dt.$$

Where we can use that

$$\int_0^\tau j(t) dt = -\frac{1}{\alpha} \ln \left(\frac{\beta(a_0)}{\beta(a_0) + \alpha j_0(e^{\beta(a_0)\tau} - 1)} \right).$$

Thus we obtain the end of season birth potential of

$$b(1) = \theta\beta(a_0)a_0 + \theta a_0 \ln \left(\frac{\beta(a_0)}{\beta(a_0) + \alpha j_0(e^{\beta(a_0)} - 1)} \right). \quad (4.4)$$

Here $\theta\beta(a_0)a_0$ gives the maximal birth potential that is generated from a certain adult population a_0 when there are no juveniles during a season (and thus do not consume any resource).

Projection of the non-growing season onto next growing seasons initial state Now we have obtained the end of season states from the initial conditions of a_0 and j_0 . Thus the continuous part of the dynamics as in (3.1) is summarised by

$$C \begin{pmatrix} \bar{r}(a_0, j_0) \\ j_0 \\ a_0 \\ 0 \end{pmatrix} = \begin{pmatrix} \bar{r}(a(1), j(1)) \\ \frac{\beta(a_0)j_0e^{\beta(a_0)}}{\alpha j_0e^{\beta(a_0)} + \beta(a_0) - \alpha j_0} \\ a_0 \\ \theta\beta(a_0)a_0 + \theta a_0 \ln \left(\frac{\beta(a_0)}{\beta(a_0) + \alpha j_0(e^{\beta(a_0)} - 1)} \right) \end{pmatrix}. \quad (4.5)$$

At the end of the season the projection onto the next seasons initial states takes place. This was given by (3.11) for the case of seasonal death of the species.

Applying this to (4.5) gives

$$\begin{aligned}
P \left(C \begin{pmatrix} \bar{r}(a_n(0), j_n(0)) \\ j_n(0) \\ a_n(0) \\ 0 \end{pmatrix} \right) &= \begin{pmatrix} \bar{r}(a_{n+1}(0), j_{n+1}(0)) \\ \frac{\mu_d}{\theta} b_n(1) \\ \mu_d a_n(0) + \mu_d \theta j_n(1) \\ 0 \end{pmatrix} \\
&= \begin{pmatrix} \bar{r}(a_{n+1}(0), j_{n+1}(0)) \\ \frac{\mu_d}{\theta} \left(\theta \beta(a_n(0)) a_n(0) + \theta a_n(0) \ln \left(\frac{\beta(a_n(0))}{\beta(a_n(0)) + \alpha j_n(0) (e^{\beta(a_n(0))} - 1)} \right) \right) \\ \mu_d a_n(0) + \mu_d \theta \frac{\beta(a_n(0)) j_n(0) e^{\beta(a_n(0))}}{\alpha j_n(0) e^{\beta(a_n(0))} + \beta(a_n(0)) - \alpha j_n(0)} \\ 0 \end{pmatrix}. \tag{4.6}
\end{aligned}$$

Here we use the subscripts to mark which season the states belong to.

We can now see that the system which contains the interesting dynamics reduces to a two-dimensional map for the initial states of the species from season to season. We shall call this map $A : \mathbb{R}^2 \rightarrow \mathbb{R}^2$ with

$$\begin{pmatrix} j_n \\ a_n \end{pmatrix} \mapsto \begin{pmatrix} \mu_d \beta(a_n) a_n + \mu_d a_n \ln \left(\frac{\beta(a_n)}{\beta(a_n) + \alpha j_n (e^{\beta(a_n)} - 1)} \right) \\ \mu_d a_n + \mu_d \theta \frac{\beta(a_n) j_n e^{\beta(a_n)}}{\beta(a_n) + \alpha j_n (e^{\beta(a_n)} - 1)} \end{pmatrix}, \tag{4.7}$$

where we had

$$\begin{aligned}
\alpha &= \frac{\delta}{\rho}, \\
\beta(a_n) &= \delta - \frac{\delta}{\rho} a_n - q.
\end{aligned}$$

4.1.2 Stability analysis

Transcritical bifurcation of zero-steady state We start by observing that the system in (4.7) always has a fixed point at zero. To be able to determine the stability of this point we compute the Jacobian matrix $J_{(j,a)} =$

$$\begin{pmatrix} -\mu_d a \left(\frac{\alpha(e^{\beta(a)} - 1)}{\beta(a) + \alpha j(e^{\beta(a)} - 1)} \right) & \mu_d (\delta - q - 2\alpha a) + \mu_d \ln \left(\frac{\beta(a)}{\beta(a) + \alpha j(e^{\beta(a)} - 1)} \right) + \mu_d a \left(\frac{\alpha^2 j ((1 - \beta(a)) e^{\beta(a)} - 1)}{\beta(a) (\beta(a) + \alpha j(e^{\beta(a)} - 1))} \right) \\ \mu_d \theta \left(\frac{\beta(a)^2 e^{\beta(a)}}{(\beta(a) + \alpha j(e^{\beta(a)} - 1))^2} \right) & \mu_d - \mu_d \theta \left(\frac{j \alpha e^{\beta(a)} (\beta(a)^2 + \alpha j (e^{\beta(a)} - \beta(a) - 1))}{(\beta(a) + \alpha j(e^{\beta(a)} - 1))^2} \right) \end{pmatrix}. \tag{4.8}$$

Which in the point $(0, 0)$ simplifies to

$$J_{(0,0)} = \begin{pmatrix} 0 & \mu_d \beta(0) \\ \mu_d \theta e^{\beta(0)} & \mu_d \end{pmatrix}. \tag{4.9}$$

The point $(0, 0)$ is stable if and only if both eigenvalues corresponding to $J_{(0,0)}$ have absolute values smaller than 1. From (4.9) we compute the eigenvalues

$$\lambda_{1,2} = \frac{\mu_d}{2} \left(1 \pm \sqrt{1 + 4\theta\beta(0)e^{\beta(0)}} \right),$$

where we see that if we assume $\beta(0) = \delta - q > 0$ these are always real valued and we have the ordering $\lambda_1 < \lambda_2$ with λ_1 corresponding to the negative sign and λ_2 to the positive sign in the expression. This gives the condition for stability of

$$-1 < \frac{\mu_d}{2} \left(1 - \sqrt{1 + 4\theta\beta(0)e^{\beta(0)}} \right), \quad \text{and} \quad \frac{\mu_d}{2} \left(1 + \sqrt{1 + 4\theta\beta(0)e^{\beta(0)}} \right) < 1.$$

When we rewrite these we find this constitutes

$$\frac{\mu_d^2 \theta \beta(0) e^{\beta(0)}}{1 + \mu_d} < 1, \quad \text{and} \quad \frac{\mu_d^2 \theta \beta(0) e^{\beta(0)}}{1 - \mu_d} < 1, \quad (4.10)$$

where, since $0 < \mu_d < 1$, the second is violated before the first. When the corresponding eigenvalue moves through the unit circle it will cause a transcritical bifurcation.

Numerical analysis of Neimark-Sacker bifurcation For further analysis of the bifurcations we can get we shall resort to numerical analysis, since the other fixed points can not be explicitly calculated. To do this we use the *xpp* and *AUTO* packages. These allow for the creation of numerical bifurcation portraits for given parameter values by continuation from a known fixed point.

We consider the bifurcations created by varying the parameters θ and δ , these determine the 'balance' between juvenile and adult population and efficiency of the species respectively.

For creating the bifurcation diagrams we use the following code, where this one was used for creating figure 4.2-A.

```
p theta=0.1, delta = 0.5, rho=40, q=0.01, mu=0.5
init a=0, j=0
j(t+1)=mu/theta*(delta*theta*a-a*q-a^2*delta*theta/rho
           -a*theta*log((delta-q-a*delta/rho)/
           (delta-q-a*delta/rho
           +(exp(delta-q-a*delta/rho)-1)*j*delta/(rho))))
a(t+1)=mu*a+exp(delta-q-a*delta/rho)*j*theta*mu
           *(delta-q-a*delta/rho)/
           (delta-q-a*delta/rho
           +(exp(delta-q-a*delta/rho)-1)*j*delta/(rho))
```

```

@ meth=discrete , total=100,njmp=1
@ autoxmin=1,autoxmax=21,autoymin=-2,autoymax=4
@ dsmax=.5,dsmin=.000001,parmin=1,parmax=20
done

```

In figure 4.2 we can see the transcritical bifurcation when 0 becomes unstable, from this a stable non-trivial solution appears. We find this non-trivial solution can lose stability through a Neimark-Sacker bifurcation when θ , δ or μ_d gets bigger. This is also illustrated in figure 4.4 where we plot an iteration of the map A for different parameter values.

We also learn that for a higher survival probability μ_d the steady state value of the juvenile population can actually decrease. This is a consequence of the fact that when the survival probability for the adult population increases the number of juveniles needed to keep the population at steady state is lower. This result of lower death rate leading to decreased population may seem counterintuitive but can be seen as a result of the carrying capacity of the resource being reached and therefore restricting further growth of the population.

In figure 4.3 we also show the two parameter plane in which we find three areas of qualitative behaviour. In area 1 zero is the stable steady state, in area 2 there exists a non-trivial stable steady state and in area 3 both steady states are unstable and an invariant curve with more complex behaviour is present.

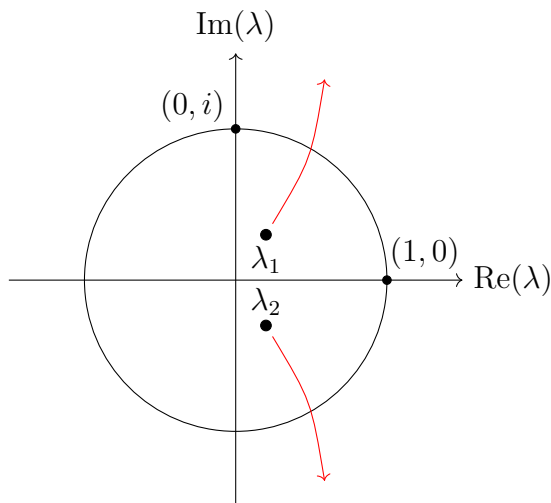


Figure 4.1: Eigenvalue picture

Geometric analysis of the non-trivial equilibrium Since we can not solve the non-trivial steady state explicitly, we will focus on investigating the dynamics

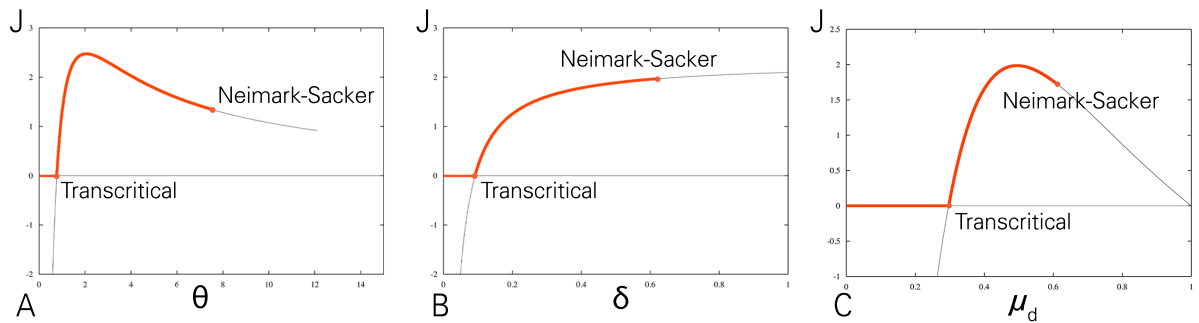


Figure 4.2: Two bifurcation diagrams of the map A in (4.7), A varying θ , B varying δ and C varying μ_d . The red parts of the curves represent the stable solutions whereas the black parts represent the unstable solutions. The parameter values used were $\rho = 40, q = 0.01, \mu_d = 0.5, \delta = 0.5, \theta = 10$.

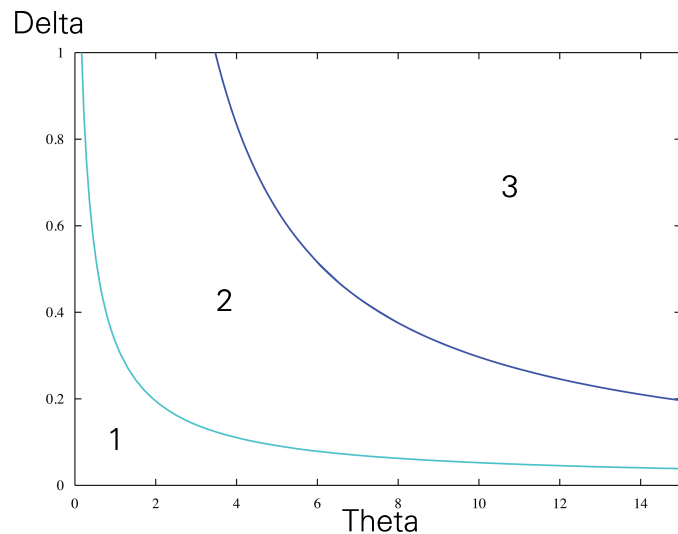


Figure 4.3: Two parameter bifurcation diagram of the map A in (4.7), varying δ and θ . The parameter values used were $\rho = 40, q = 0.01, \mu_d = 0.5$.

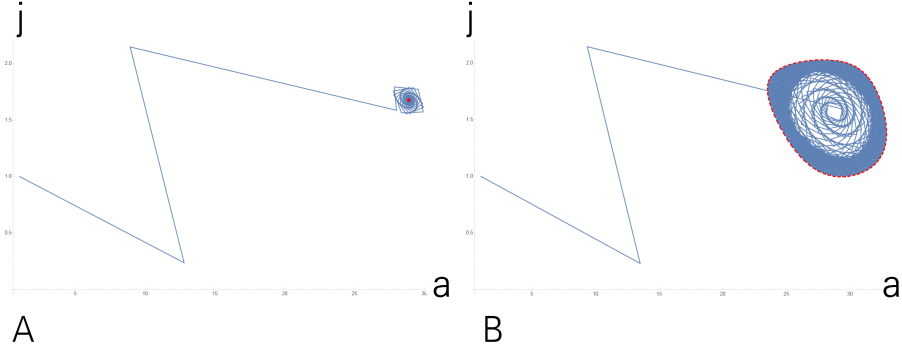


Figure 4.4: A and B show the positive semi-orbit of the point $(1,1)$ under iteration of the map A in (4.7). For the parameter values in A we find an attracting non-trivial equilibrium point whereas in B an attracting limit cycle appears, both are visualised in red. The parameter values used are $\delta = 0.5, \rho = 40, q = 0.01$ and $\mu_d = 0.5$, and $\theta = 15.5$ for A, and $\theta = 16.4$ for B.

of (4.7) visually. We will study both the map $j_{n+1}(j_n, a_n)$ and $a_{n+1}(j_n, a_n)$ of A separately, trying to found out the domain of the steady state and give some insight into the corresponding dynamics.

First of all, we observe that the map $j_{n+1}(j_n, a_n)$ is bounded from above by $\mu_d\beta(a_n)a_n$ since $\frac{\beta(a_n)}{\beta(a_n) + \alpha j_n(e^{\beta(a_n)} - 1)} \leq 1$ if $a_n > 0$ and $j_n > 0$ as assumed. Thus we have

$$\mu_d a_n \ln \left(\frac{\beta(a_n)}{\beta(a_n) + \alpha j_n(e^{\beta(a_n)} - 1)} \right) < 0.$$

This gives the upper bound

$$j_{n+1} \leq \mu_d \beta(a_n) a_n \quad (4.11)$$

Now to compute the maximum possible value of j_{n+1} we set $\frac{d}{da_n} \mu_d \beta(a_n) a_n = 0$ and find the maximum is given at $a_n^* = \frac{\delta - q}{2\alpha}$. This gives

$$j_{n+1} \leq \mu_d \beta(a_n^*) a_n^* = \frac{\mu_d(\delta - q)^2}{4\alpha} < \frac{\delta\rho}{4}.$$

Also, if we try to solve $j_{n+1}(j_n, a_n) = 0$ we find that either $a_n = 0$ or

$$\begin{aligned} \beta(a_n) &= -\ln \left(\frac{\beta(a_n)}{\beta(a_n) + \alpha j_n(e^{\beta(a_n)} - 1)} \right) \\ &= \ln \left(1 - \frac{\alpha j_n}{\beta(a_n)} + \frac{\alpha j_n}{\beta(a_n)} e^{\beta(a_n)} \right). \end{aligned}$$

And thus if $\frac{\alpha j_n}{\beta(a_n)} = 1$ we have

$$\ln \left(1 - \frac{\alpha j_n}{\beta(a_n)} + \frac{\alpha j_n}{\beta(a_n)} e^{\beta(a_n)} \right) = \ln (1 - 1 + e^{\beta(a_n)}) = \ln (e^{\beta(a_n)}) = \beta(a_n).$$

Thus another solution is given by $\alpha j_n = \beta(a_n)$, which gives

$$j_n + a_n = \rho - \frac{\rho q}{\delta}.$$

This means all positive solutions will be on the domain $a_n > 0, j_n > 0$ and $j_n + a_n < \rho - \frac{\rho q}{\delta}$. This last condition also ensures that the quasi-steady state of the resource is positive. In figure 4.5 these different results can be observed by viewing the function $j_{n+1}(j_n, a_n)$ as a function of the different variables.

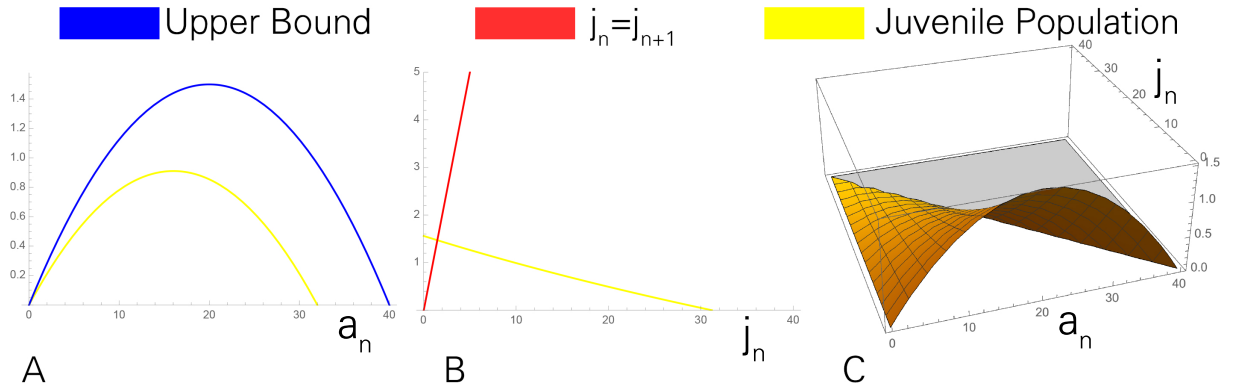


Figure 4.5: A: j_{n+1} as a function of a_n together with the upper bound (4.11). B: j_{n+1} as a function of j_n . C: A 3d-visualisation of $j_{n+1}(j_n, a_n)$. Parameter values $\delta = 0.5, \rho = 40, \theta = 5, q = 0.01, \mu_d = 0.5$.

Next we focus on the map $a_{n+1}(j_n, a_n)$. We have already derived the bound

$\alpha a < \delta - q - \alpha j$ which we will use here. We observe that

$$\begin{aligned}
a_{n+1}(j_n, a_n) &= \mu_d a_n + \mu_d \theta \frac{\beta(a_n) j_n e^{\beta(a_n)}}{\beta(a_n) + \alpha j_n (e^{\beta(a_n)} - 1)} \\
&= \mu_d a_n + \mu_d \theta \frac{\beta(a_n) j_n e^{\beta(a_n)}}{\delta - q - \alpha a + \alpha j_n (e^{\beta(a_n)} - 1)} \\
&< \mu_d a_n + \mu_d \theta \frac{\beta(a_n) j_n e^{\beta(a_n)}}{\delta - q - (\delta - q - \alpha j_n) + \alpha j_n (e^{\beta(a_n)} - 1)} \\
&= \mu_d a_n + \mu_d \theta \frac{\beta(a_n) j_n e^{\beta(a_n)}}{\alpha j_n e^{\beta(a_n)}} \\
&= \mu_d a_n + \mu_d \theta \frac{\beta(a_n)}{\alpha}.
\end{aligned} \tag{4.12}$$

From this we can compute the stable point of $x_{n+1} = \mu_d x_n + \mu_d \theta \frac{\beta(x_n)}{\alpha}$, which gives

$$\bar{x} = \frac{\mu_d \theta}{1 - \mu_d + \mu_d \theta} \frac{\delta - q}{\alpha} < \frac{\delta - q}{\alpha}.$$

Thus since we have $a_{n+1}(j_n, 0) > 0$ for $j_n > 0$ and $a_{n+1}(j_n, \bar{x}) < \bar{x}$ there exist an \bar{a} in between such that $a_{n+1}(j_n, \bar{a}) = \bar{a}$. Thus we conclude that $0 < \bar{a} < \frac{\delta - q}{\alpha}$.

We can also easily see that a_{n+1} is an increasing function in terms of j_n since we can write

$$a_{n+1}(j_n, a_n) = \mu_d a_n + \mu_d \theta \frac{\beta(a_n) e^{\beta(a_n)}}{\frac{\beta(a_n)}{j_n} + \alpha (e^{\beta(a_n)} - 1)},$$

which gives

$$\frac{\partial a_{n+1}(j_n, a_n)}{\partial j_n} = \mu_d \theta \left(\frac{\beta(a)^2 e^{\beta(a)}}{(\beta(a) + \alpha j (e^{\beta(a)} - 1))^2} \right) > 0. \tag{4.13}$$

In figure 4.6 we show the behaviour of a_{n+1} as a function of the different variables.

In addition figure 4.7 shows the domain we have derived for the non-trivial equilibrium (\bar{j}, \bar{a}) . From this we learn that the assumption of no starvation is satisfied for (j, a) . Since we have $\bar{j} < \beta(\bar{a})/\alpha$ and by the carrying capacity of the logistic equation this gives for the juvenile population during the entire growing season $\bar{j}(t) < \beta(\bar{a})/\alpha$ for all $t > 0$. Therefore, for the resource we obtain $\bar{r}(t) = 1 - \frac{j(t) + a(t)}{\rho} > q/\delta$ implying the no starvation condition $\delta \bar{r}(t) - q > 0$ is satisfied. However, this does not mean that no starvation is possible for the invariant curve beyond the Neimark-Sacker bifurcation since this might expand outside of the domain.

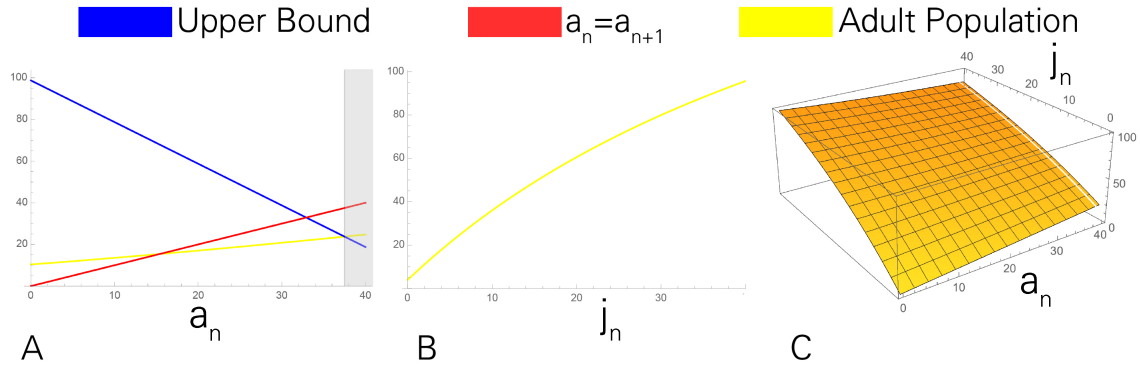


Figure 4.6: A: a_{n+1} as a function of a_n together with the upper bound (4.12) on the domain $0 < a_n < \rho - j_n$ and the line $a_n = a_{n+1}$. B: a_{n+1} as a function of j_n . C: A 3d-visualisation of $a_{n+1}(j_n, a_n)$. Parameter values $\delta = 0.5, \rho = 40, \theta = 5, q = 0.01, \mu_d = 0.5$.

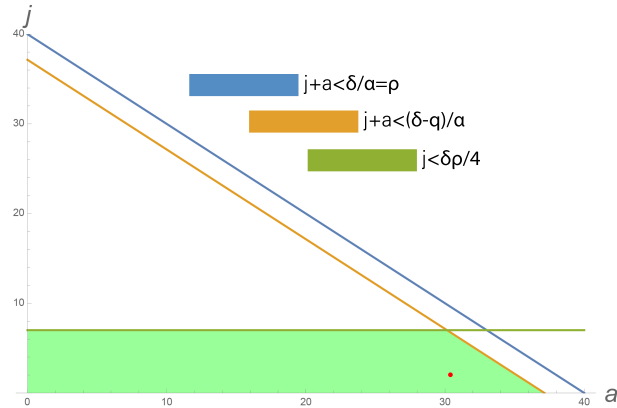


Figure 4.7: A representation of the domain of the non-trivial equilibrium (\bar{j}, \bar{a}) .

Existence of the non-trivial steady state To show when a positive non-trivial steady state exists we first show there exist two functions giving the unique solution to $a_{n+1}(j_n, a_n) = a_n$ for every j_n and $j_{n+1}(j_n, a_n) = j_n$ for every a_n . For the first we need to show that $\frac{\partial^2 a_{n+1}}{\partial a_n^2} > 0$. The second is clear since $j_{n+1}(j_n, a_n)$ is decreasing in j_n and $j_{n+1}(0, a_n) > 0$. In this section we will always be assuming $a + j < \frac{\delta-q}{\alpha}$ as we have derived.

We will first show that $\frac{\partial^2 a_{n+1}}{\partial a_n^2} > 0$. We have that

$$\frac{\partial^2 a_{n+1}}{\partial a_n^2} = -\mu_d \theta \frac{j \alpha^2 e^{\beta(a)} (\beta(a) + \alpha j (e^{\beta(a)} - 1))}{(\beta(a) + \alpha j (e^{\beta(a)} - 1))^4} N_1 > 0,$$

where

$$N_1 = -\beta(a)^3 - \alpha^2 j^2 \underbrace{(2 + \beta(a) + e^{\beta(a)}(\beta(a) - 2))}_{>0} + \underbrace{\alpha j (e^{\beta(a)}(\beta(a)^2 - 4\beta(a) + 2) + 2(\beta(a)^2 + \beta(a)))}_{<0} < 0,$$

and

$$(\beta(a) + \alpha j (e^{\beta(a)} - 1)) = \delta - q - \alpha(a + j) + \alpha j e^{\beta(a)} > 0 \quad \text{since } a + j < \frac{\delta - q}{\alpha}.$$

Now since we have $a_{n+1}(j_n, 0) > 0$ and $a_{n+1}(j_n, \frac{\delta-q}{\alpha}) < \frac{\delta-q}{\alpha}$ and supposing there are two points $0 < x_1 < x_2 < \frac{\delta-q}{\alpha}$ such that $a_{n+1}(j_n, x_1) = a_{n+1}(j_n, x_2) = a_n$. Then we must have $\frac{\partial a_{n+1}(x_2)}{\partial a_n} > 1$, thus by $\frac{\partial^2 a_{n+1}}{\partial a_n^2} > 0$ this gives $\frac{\partial a_{n+1}(x)}{\partial a_n} > 1$ for all $x > x_2$. Therefore, $a_{n+1}(j_n, x) > a_n$ for all $x > x_2$ which gives $a_{n+1}(j_n, \frac{\delta-q}{\alpha}) > \frac{\delta-q}{\alpha}$ which is a contradiction.

We now have shown that for all $0 < j_n < \frac{\delta-q}{\alpha}$ we have that $a_{n+1}(j_n, a_n) = a_n$ has a unique positive solution and for all $0 < a_n < \frac{\delta-q}{\alpha}$ we have that $j_{n+1}(j_n, a_n) = j_n$ has a unique positive solution. However, this does not necessarily imply there is a solution to $Ax = x$ in (4.7).

Let us consider the implicit functions

$$F(a, j) = j_{n+1}(j, a) - j = 0, \quad \text{and} \quad G(a, j) = a_{n+1}(j, a) - a = 0.$$

From the previous we know that these have a unique solution as functions from a to j and j to a respectively. Now for the steady state solution \bar{j} in F we have that

$$\frac{\partial \bar{j}}{\partial a} = -\frac{\partial F(\bar{j}, a)/\partial a}{\partial F(\bar{j}, a)/\partial \bar{j}},$$

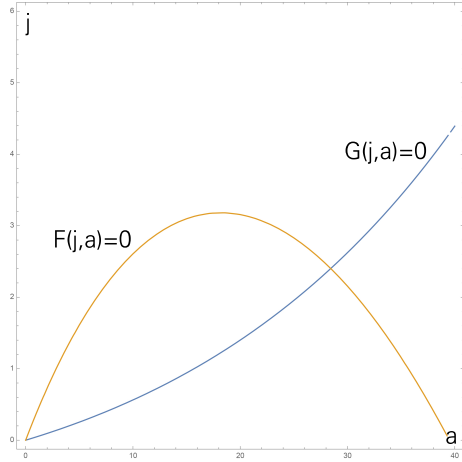


Figure 4.8: Plot of the implicit functions $F(j, a) = 0$ and $G(j, a) = 0$. These give the steady state solution of the map A in (4.7).

and for the steady state solution \bar{a} in G we have that

$$\frac{\partial j}{\partial \bar{a}} = -\frac{\partial G(j, \bar{a})/\partial \bar{a}}{\partial G(j, \bar{a})/\partial j} = -\frac{\partial a_{n+1}(j, \bar{a})/\partial \bar{a} - 1}{\partial a_{n+1}(j, \bar{a})/\partial j} > 0,$$

since

$$\partial a_{n+1}(j, \bar{a})/\partial \bar{a} - 1 = \underbrace{\mu_d - 1}_{<0} - \underbrace{\mu_d \theta \left(\frac{j \alpha e^{\beta(a)} (\beta(a)^2 + \alpha j (e^{\beta(a)} - \beta(a) - 1))}{(\beta(a) + \alpha j (e^{\beta(a)} - 1))^2} \right)}_{>0} < 0,$$

and $\partial a_{n+1}(j, \bar{a})/\partial j > 0$ as seen in (4.13). Thus the solution to G is increasing as a function of a . In combination with $F(a, 0) = 0$ for $a = 0$ and $a = \frac{\delta-q}{\alpha}$ this gives the situation in figure 4.8.

First of all we observe that

$$-\frac{\partial F(0, 0)/\partial \bar{a}}{\partial F(0, 0)/\partial j} = \beta(0)\mu_d, \quad -\frac{\partial G(0, 0)/\partial \bar{a}}{\partial G(0, 0)/\partial j} = \frac{1 - \mu_d}{\mu_d \theta e^{\beta(0)}},$$

thus F is steeper than G in $(0, 0)$ when $\frac{\mu_d^2 \theta \beta(0) e^{\beta(0)}}{1 - \mu_d} > 1$. This coincides with the instability of the trivial solution in (4.10). In this case the existence of a positive non-trivial solution is ensured.

To prove uniqueness of the non trivial steady state we would also need to prove that the second derivative of the solution to F is negative and the second derivative to the solution of G is positive. This however remains uncertain while it is evident from the plot for set parameter values.

Non-strong resonance in the Neimark-Sacker bifurcation To be able to ensure the existence of a limit cycle for a discrete map through a Neimark-Sacker bifurcation we must rule out the possibility of strong-resonance. In contrast to the continuous case of a Hopf bifurcation, which can be seen as the continuous counterpart of the Neimark-Sacker bifurcation, in this discrete case it is possible that instead of an invariant curve a periodic solution that is not on the invariant curve appears [24]. This can only happen when the eigenvalues of the system cross the unit circle at a specific point, being with an angle of $\frac{\pi}{2}, \frac{2\pi}{3}, \pi$ or 2π . Where π actually represents a period doubling bifurcation and 2π represents a saddle-node bifurcation. We will derive a condition under which this can not happen by showing the eigenvalues cross the unit circle in the right half-plane.

First of all observe that if the eigenvalues of a 2×2 matrix are complex, then the real part is completely determined by the trace of the matrix. Thus what we want to show is that the trace of the jacobian matrix (4.8) is positive. We can rewrite this condition as

$$\begin{aligned} -\mu_d a \left(\frac{\alpha(e^{\beta(a)} - 1)}{\beta(a) + \alpha j(e^{\beta(a)} - 1)} \right) + \mu_d - \mu_d \theta \left(\frac{j \alpha e^{\beta(a)} (\beta(a)^2 + \alpha j(e^{\beta(a)} - \beta(a) - 1))}{(\beta(a) + \alpha j(e^{\beta(a)} - 1))^2} \right) > 0, \\ \left(1 - a \left(\frac{\alpha(e^{\beta(a)} - 1)}{\beta(a) + \alpha j(e^{\beta(a)} - 1)} \right) - \theta \left(\frac{j \alpha e^{\beta(a)} (\beta(a)^2 + \alpha j(e^{\beta(a)} - \beta(a) - 1))}{(\beta(a) + \alpha j(e^{\beta(a)} - 1))^2} \right) \right) > 0, \\ \frac{a \alpha (e^{\beta(a)} - 1)}{\beta(a) + \alpha j(e^{\beta(a)} - 1)} + \theta \left(\frac{j \alpha e^{\beta(a)} (\beta(a)^2 + \alpha j(e^{\beta(a)} - \beta(a) - 1))}{(\beta(a) + \alpha j(e^{\beta(a)} - 1))^2} \right) < 1. \end{aligned}$$

Using that on the domain of the non-trivial steady state $\beta(a) + \alpha j(e^{\beta(a)} - 1) > \beta(a)$ and $e^{\beta(a)} - \beta(a) - 1 = \frac{\beta(a)^2}{2} + \mathcal{O}(\beta(a)^3) \approx \frac{\beta(a)^2}{2}$ by $0 < \beta(a) < \delta < 1$ we can simplify this condition to

$$\frac{a \alpha (e^{\beta(a)} - 1)}{\beta(a)} + \theta \alpha j e^{\beta(a)} \left(1 + \frac{\alpha j}{2} \right) < 1.$$

This is easiest to write in terms of a condition on j as

$$\alpha j \left(1 + \frac{\alpha j}{2} \right) < \frac{\beta(0) - a \alpha e^{\beta(a)}}{\theta \beta(a) e^{\beta(a)}},$$

from which we can derive that on part of the domain for (\bar{j}, \bar{a}) this condition is satisfied.

In figure 4.9 we added this condition to the domain, which is in general not completely covered. Therefore, we can not conclude the steady state does not exhibit a strong resonance in general. However, we found all solutions tried satisfy this condition but since we do not have an explicit solution we cannot check whether this is always the case.

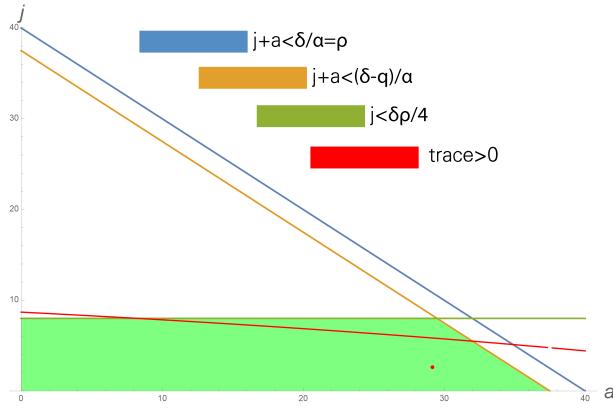


Figure 4.9: A representation of the domain of the non-trivial equilibrium (\bar{j}, \bar{a}) together with the condition for non-strong resonance.

Arnold tongues and location of the strong resonance From the numerical bifurcation analysis we find that outside the domain of the parameters ($\delta > 1$) we can show that a bifurcation through the $1 : 4$ resonance takes place. This happens when the eigenvalues cross the unit circle through i and $-i$ as in figure 4.10. At this point the bifurcation can be more complex and an invariant curve might not exist. This behaviour can be found in Kuznetsov [24]. We have found no results such that this resonance exists inside the parameter domain as is also illustrated in the previous section.

In addition to the strong resonance, periodic behaviour can appear through so-called Arnold tongues. Further away from the bifurcation the solution might enter a region in which there exists an attracting periodic solution on the invariant curve. This behaviour was first discovered by Arnold [23] and the tongues can be thought of as pictured in figure 4.12. In these tongues a periodic orbit is found, whereas outside the tongues a dense orbit on the invariant curve exists. Depending on the resonance from which the Arnold tongue materialises the period of the solution differs.

In figure 4.11 two such solutions are shown for a period 4 and period 9 solution with rotation numbers $1/4$ and $2/9$. The rotation number belonging to the invariant curve just past the bifurcation decreases when following the bifurcation down in figure 4.12. Thus the Arnold tongue belonging to the period 9 solution initiates lower on the bifurcation curve than the tongue belonging to the period 4 solution.

This shows not only dense orbits on the invariant curve but also completely periodic solutions can be found in the model when the solution moves away from the bifurcation. Since the periodic behaviour occurs over substantial regions of parameter space they are very robust against perturbations and thus are also a

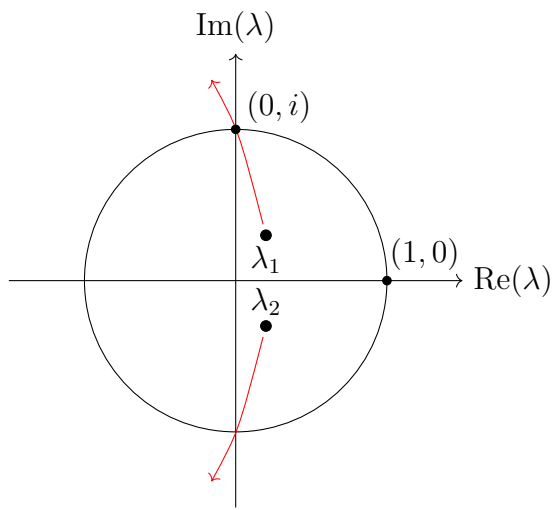


Figure 4.10: Eigenvalue picture of the complex conjugate pair of eigenvalues crossing the unit circle through the $1 : 4$ resonance.

very robust explanation for cyclic behaviour.

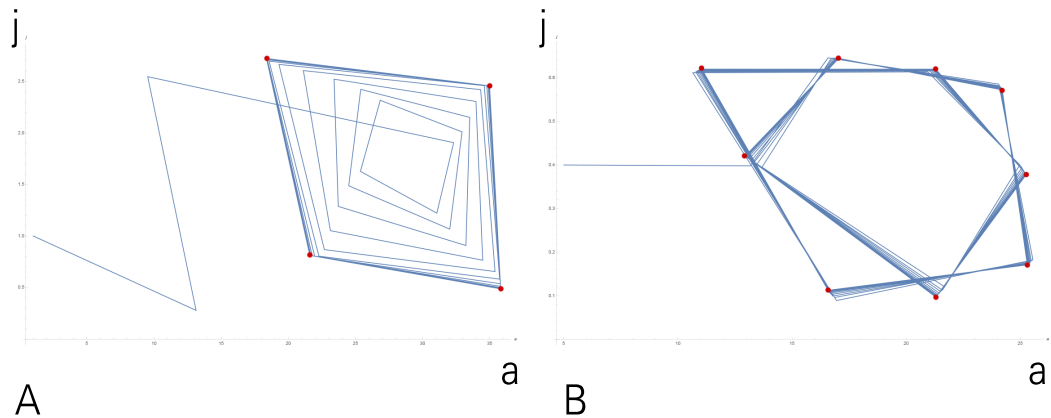


Figure 4.11: Periodic solutions of the map A in (4.7) inside the $1 : 4$ (A) and $2 : 9$ (B) Arnold tongues.

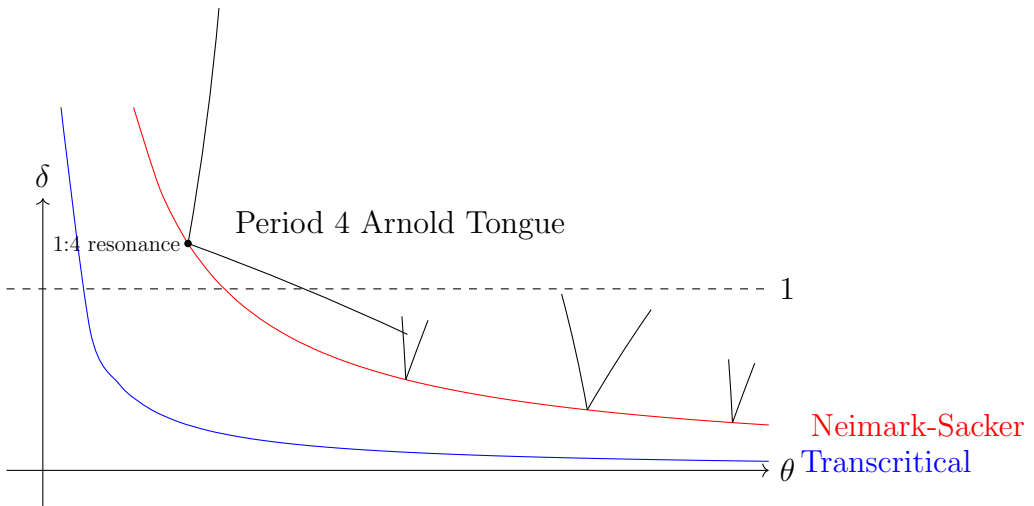


Figure 4.12: Sketch of how the Arnold tongues are situated in the bifurcation plane.

Inside the Arnold tongues a periodic solution exists, in the remaining area after the Neimark-Sacker bifurcation a dense almost periodic orbit on the invariant curve exists. The Arnold tongue coming from the $1 : 4$ resonance gives a period 4 solution inside the corresponding Arnold tongue.

4.2 Logistic resource with continuous death

In this section we consider the model where resource dynamics is governed logistically, like in the previous section. However, death is modelled during the growing season instead of the non-growing season. This corresponds to a situation where seasonality is only present in the birth process. We show how to derive the discrete season to season map for this model and compare its dynamics to the model with discrete death (so during the non-growing season).

4.2.1 Solving the continuous growing season dynamics

Solving the adult differential equation The equation for the growing season of the adult population is the simplest of the three equations to solve. The equation is given by

$$\frac{\partial a(\tau)}{\partial \tau} = -\mu_c a(\tau). \quad (4.14)$$

The equation is easily solved using the separation of variables technique and with the initial condition $a(0) = a_0$ gives the solution

$$a(\tau) = a_0 e^{-\mu_c \tau}. \quad (4.15)$$

We will use this solution in solving the other two differential equations.

Solving the juvenile differential equation For the juvenile growing season we have derived a second order differential equation with variable coefficients, in contrast to equation (4.1) where we had a constant coefficient equation. Now the dynamics of the juvenile population are given by

$$\frac{\partial j(\tau)}{\partial \tau} = -\frac{\delta}{\rho} j(\tau)^2 + \left(\delta - \frac{\delta}{\rho} a_0 e^{-\mu_c \tau} - q - \mu_c \right) j(\tau). \quad (4.16)$$

This particular system we can recognise as a Bernoulli differential equation which can be solved by first rewriting it and then using an integrating factor. First for ease of notation we write, using $f(\tau) := -\delta + \frac{\delta}{\rho} a_0 e^{-\mu_c \tau} + q + \mu_c$,

$$\frac{\partial j(\tau)}{\partial \tau} + f(\tau)j(\tau) = -\frac{\delta}{\rho} j(\tau)^2. \quad (4.17)$$

Now let $g(\tau) = j(\tau)^{-1}$, then we get $\frac{\partial g(\tau)}{\partial \tau} = -j(\tau)^{-2} \frac{\partial j(\tau)}{\partial \tau}$. Thus by

$$j(\tau)^{-2} \frac{\partial j(\tau)}{\partial \tau} = -\frac{\delta}{\rho} - f(\tau)j(\tau)^{-1} = -\frac{\delta}{\rho} - f(\tau)g(\tau)$$

we rewrite (4.17) as

$$\frac{\partial g(\tau)}{\partial \tau} = \frac{\delta}{\rho} + f(\tau)g(\tau).$$

This is a linear ordinary differential equation which can be solved using an integrating factor to give, for a constant c_2 and $\tau \geq 0$,

$$g(\tau) = \frac{c_2 + \int_0^\tau \frac{\delta}{\rho} e^{-\int_0^x f(y) dy} dx}{e^{-\int_0^\tau f(x) dx}}$$

with $-\int_0^\tau f(x) dx = (\delta - q - \mu_c)\tau + \frac{\delta a_0}{\rho \mu_c} (e^{-\mu_c \tau} - 1)$, and thus we find as a solution for $j(\tau)$ that

$$j(\tau) = g(\tau)^{-1} = \frac{e^{(\delta-q-\mu_c)\tau + \frac{\delta a_0}{\rho \mu_c} (e^{-\mu_c \tau} - 1)}}{c_2 + \int_0^\tau \frac{\delta}{\rho} e^{(\delta-q-\mu_c)x + \frac{\delta a_0}{\rho \mu_c} (e^{-\mu_c x} - 1)} dx}, \quad (4.18)$$

and we compute that for $j(0) = j_0$ we have $c_2 = \frac{1}{j_0}$.

Solving the birth potential differential equation The last equation of the growing season gives the birth potential dynamics. It is given by

$$\frac{\partial b(\tau)}{\partial \tau} = \delta\theta \left(1 - \frac{j(\tau) + a_0 e^{-\mu_c \tau}}{\rho} \right) a_0 e^{-\mu_c \tau} - q\theta a_0 e^{-\mu_c \tau} - \mu_c b(\tau). \quad (4.19)$$

To find a solution for (4.19) we rewrite it using $y(\tau) = \delta\theta \left(1 - \frac{j(\tau) + a_0 e^{-\mu_c \tau}}{\rho} \right) a_0 e^{-\mu_c \tau} - q\theta a_0 e^{-\mu_c \tau}$ to get

$$\frac{\partial b(\tau)}{\partial \tau} = y(\tau) - \mu_c b(\tau).$$

This can be solved using an integrating factor to obtain, with $b(0) = 0$,

$$\begin{aligned} b(\tau) &= e^{-\mu_c \tau} \int_0^\tau e^{\mu_c x} y(x) dx \\ &= \underbrace{(\delta - q)\theta a_0 \tau e^{-\mu_c \tau} - \frac{\delta\theta}{\mu_c \rho} a_0^2 e^{-\mu_c \tau} (1 - e^{-\mu_c \tau})}_{\text{maximal birth potential}} - \underbrace{\frac{\delta\theta}{\rho} a_0 e^{-\mu_c \tau} \int_0^\tau j(x; j_0, a_0) dx}_{\text{decrease by juvenile competition}}, \end{aligned} \quad (4.20)$$

which like (4.4) consists of two parts. The first describes the maximal birth potential from an initial adult population a_0 , which is generated when there is no competition with juveniles ($j_0 = 0$). The second part then describes how much the birth potential is decreased by competition for resource between juveniles and adults.

Deriving the discrete year to year map In the previous three sections we have derived the end of growing season states for the species. We apply the projection (3.2) to this state and we find the yearly dynamics

$$\begin{aligned} P \left(C \begin{pmatrix} \bar{r}(a_n(0), j_n(0)) \\ j_n(0) \\ a_n(0) \\ 0 \end{pmatrix} \right) &= \begin{pmatrix} \bar{r}(a_{n+1}(0), j_{n+1}(0)) \\ \frac{1}{\theta} b_n(1) \\ a_n(1) + \theta j_n(1) \\ 0 \end{pmatrix} \\ &= \begin{pmatrix} \bar{r}(a_{n+1}(0), j_{n+1}(0)) \\ (\delta - q)a_n(0)e^{-\mu_c} - \frac{\delta}{\mu_c \rho} a_n(0)^2 e^{-\mu_c} (1 - e^{-\mu_c}) - \frac{\delta}{\rho} a_n(0) e^{-\mu_c} \int_0^1 j(x; j_n(0), a_n(0)) dx \\ e^{-\mu_c} a_n(0) + \theta j_n(0) \frac{e^{(\delta - q - \mu_c) + \frac{\delta a_n(0)}{\rho \mu_c} (e^{-\mu_c} - 1)}}{1 + j_n(0) \int_0^1 \frac{\delta}{\rho} e^{(\delta - q - \mu_c)x + \frac{\delta a_n(0)}{\rho \mu_c} (e^{-\mu_c} - 1)} dx} \\ 0 \end{pmatrix}. \end{aligned} \quad (4.21)$$

From this we see the dynamics can be simplified to a two dimensional map for the juvenile and adult initial states. The map is given by $A_c : \mathbb{R}^2 \rightarrow \mathbb{R}^2$ with

$$\begin{pmatrix} j_n \\ a_n \end{pmatrix} \mapsto \begin{pmatrix} (\delta - q)a_n e^{-\mu_c} - \frac{\delta}{\mu_c \rho} a_n^2 e^{-\mu_c} (1 - e^{-\mu_c}) - \frac{\delta}{\rho} a_n e^{-\mu_c} \int_0^1 j(x; j_n, a_n) dx \\ e^{-\mu_c} a_n + \theta j_n \frac{e^{(\delta-q-\mu_c)+\frac{\delta a_n}{\rho \mu_c}(e^{-\mu_c}-1)}}{1 + j_n \int_0^1 \frac{\delta}{\rho} e^{(\delta-q-\mu_c)x+\frac{\delta a_n}{\rho \mu_c}(e^{-\mu_c x}-1)} dx} \end{pmatrix}. \quad (4.22)$$

In the next section we will analyse the dynamics of this map A_c .

4.2.2 Stability analysis

Bifurcation of the trivial steady state We can easily see that $(0, 0)$ is a steady state of the map A_c . We call this the trivial steady state since this corresponds to an extinct population. To determine stability of this point we calculate the Jacobian matrix in $(0, 0)$ and find that

$$J_{(0,0)} = \begin{pmatrix} 0 & e^{-\mu_c}(\delta - q) \\ e^{-\mu_c}\theta e^{\delta-q} & e^{-\mu_c} \end{pmatrix}. \quad (4.23)$$

This is identical to the Jacobian of the discrete death model, with the difference that we now have the survival probability $e^{-\mu_c}$ instead of the survival probability μ_d . Therefore, stability analysis will be the same as in the previous section with the conclusion that the trivial steady state $(0, 0)$ is stable when

$$\frac{e^{-2\mu_c}\theta(\delta - q)e^{\delta-q}}{1 - e^{-\mu_c}} < 1,$$

and loses stability through a transcritical bifurcation.

Numerical Bifurcation Analysis To analyse the dynamics of the non-trivial steady state of the map A_c we again resort to a numerical analysis using the programs *xpp* and *AUTO*. Since the map A_c contains two integrals which the software does not allow for, we include the calculation of the numerical integral into the code of the function. This we checked using simulation in *Mathematica* which has shown the results coincide.

The code for using the bifurcation diagrams in figures 4.13 and 4.14 is:

```
p theta=0.15, delta = 0.5, rho=40, q=0.01, mu=0.5
init a=0, j=0
f(x) = exp((delta-q-mu)*x+(delta*a/(rho*mu))*(exp(-mu*t)-1))
f2(x) = delta*exp(f(x))/rho
f3(x) = sum(0,x*1000)of(f2(i'/1000+1/1000)/1000)
```

```

Juv(x) = f(x)/(1/j+f3(x))
Adult(x) = a*exp(-mu*x)
g(x) = exp(mu*x)*(delta*theta*(1-(Juv(x)+Adult(x))/rho)
                  *Adult(x)-q*theta*Adult(x))
gInt(x) = sum(0,x*1000) of (g(i')/1000+1/1000)/1000
Birth(x) = exp(-mu*x)*gInt(x)

```

```

j(t+1)=Birth(1)/theta
a(t+1)=Adult(1)+theta*Juv(1)
@ meth=discrete , total=100,njmp=1
@ autoxmin=0,autoxmax=21,autoymin=-2,autoymax=5
@ dsmax=.5,dsmin=.000001,parmin=0.1,parmax=20
done

```

The numerical analysis in figure 4.13 shows the dynamics of the system including death into the growing season and the system including death into the non-growing season are similar. When the trivial steady state loses stability a stable non-trivial steady state materialises. This non-trivial steady state can loose stability through a Neimark-Sacker bifurcation, where a complex pair of eigenvalues crosses the unit circle, which gives rise to a closed invariant curve on which periodic behaviour can appear. This is also illustrated in figure 4.15.

In figure 4.14 we can also see the two parameter bifurcation analysis in the parameters δ and θ . This shows we can distinguish three areas, in area 1 zero is stable and thus the model leads to extinction of the species. In area 2 we have a stable non-trivial steady state to which the system converges when iterated. In area 3 both steady states are unstable and a closed invariant curve appears, this can lead to periodic or more complex behaviour on this curve. The dynamics are thus similar to those of the model with the continuous death rate set to zero.

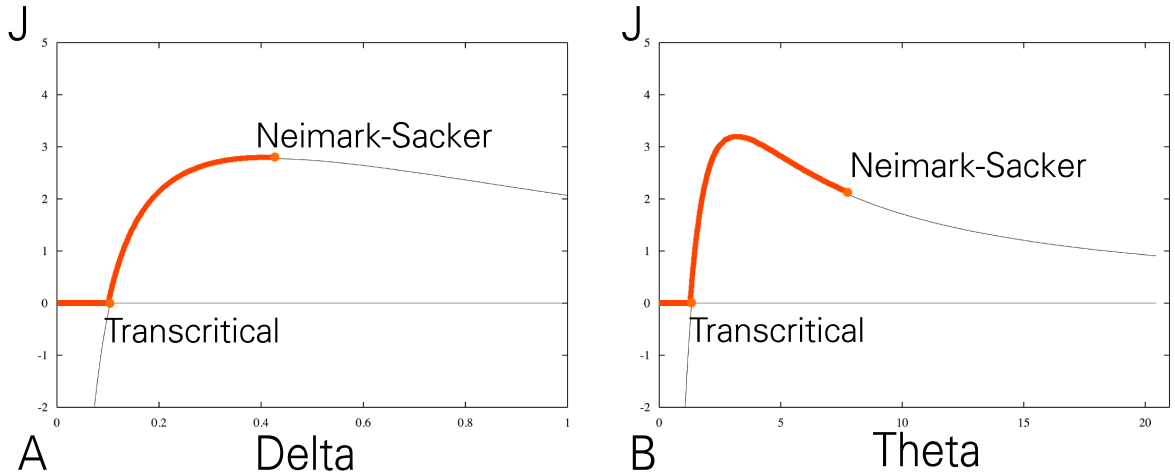


Figure 4.13: Two bifurcation diagrams of the map A_c in (4.22), A varying δ and B varying θ . The red parts of the curves represent the stable solutions whereas the black parts represent the unstable solutions. The parameter values used were $\rho = 40, q = 0.01, \mu_c = 0.5$ and $\delta = 0.5$ for A and $\theta = 6$ for B.

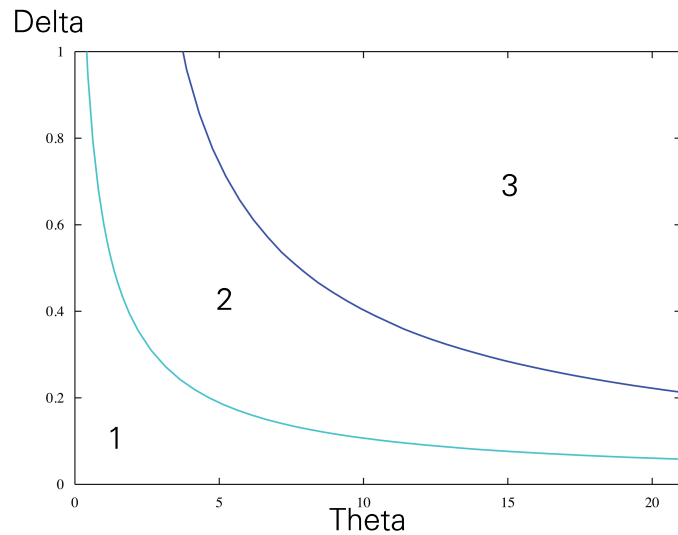


Figure 4.14: Two parameter bifurcation diagram of the map A_c in (4.22), varying δ and θ . The parameter values used were $\rho = 40, q = 0.01, \mu_c = 0.5$.

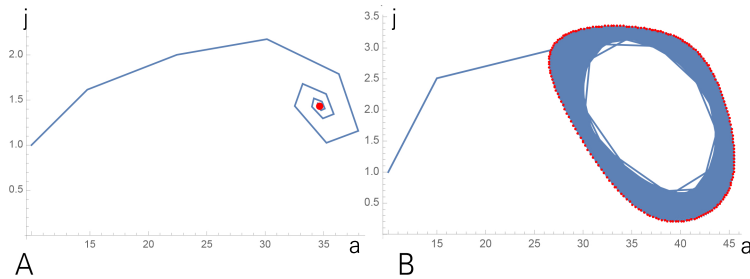


Figure 4.15: A and B show the positive semi-orbit of the point $(10,1)$ under iteration of the map A_c in (4.22). For the parameter values in A we find an attracting non-trivial equilibrium point whereas in B an attracting limit cycle appears, both are visualised in red.

4.3 Generalisation to multiple stage model

Until now we have only considered a situation where maturation of the juvenile population occurs after a single season. Clearly this reduces the applicability of the theory. Therefore, we would like to expand the idea to a model in which the maturation occurs over more than one year. We first present how to expand the model to one in which maturation occurs after two years and also present how this generalises to more than two years.

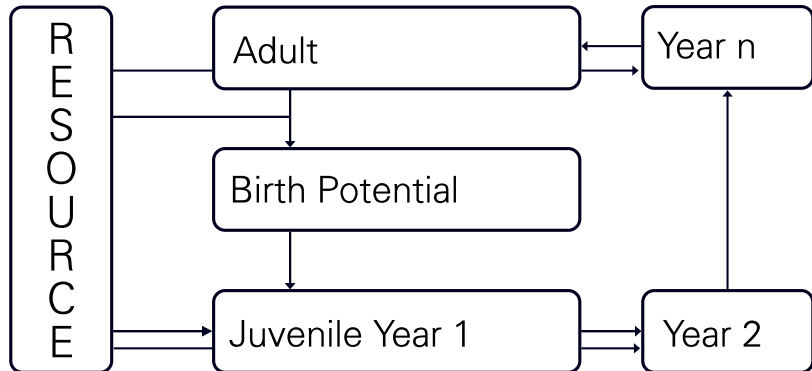


Figure 4.16: Outline of the relations between the different variables in the system when it is extended to a n -year maturation setting.

We first consider the expanded model as given in equation 4.24, which consist

of two juvenile stages (j_1 and j_2). These juvenile stages have identical growing season dynamics. For the non-growing season we have similar dynamics as we had in the models before (4.25), with the addition of a transition step from one-year juveniles to two-year juveniles. For the sake of simplicity we consider the model only containing death in the non-growing season, the procedure can similarly be applied to the model including growing season death.

We have the continuous system for the growing season with dynamics given by

$$C_{\text{2-year maturation}} : \begin{cases} \frac{\partial r}{\partial \tau} = \rho r(1 - r) - r(j_1 + j_2) - ra, \\ \frac{\partial j_1}{\partial \tau} = \delta r j_1 - q j_1, \\ \frac{\partial j_2}{\partial \tau} = \delta r j_2 - q j_2, \\ \frac{\partial a}{\partial \tau} = 0, \\ \frac{\partial b}{\partial \tau} = \delta \theta r a - q \theta a, \end{cases} \quad (4.24)$$

together with the projection for the non-growing season which becomes

$$P : \mathbb{R}^5 \rightarrow \mathbb{R}^5 \quad \text{with} \quad \begin{pmatrix} r(1) \\ j_1(1) \\ j_2(1) \\ a(1) \\ b(1) \end{pmatrix} \mapsto \begin{pmatrix} r(1) \\ \frac{\mu_d}{\theta} b(1) \\ \mu_d j_1(1) \\ \mu_d a(1) + \mu_d \theta j_2(1) \\ 0 \end{pmatrix}. \quad (4.25)$$

To be able to solve the growing season dynamics in equation 4.24 we introduce the variable j which sums up all juvenile population. Thus $j(\tau) := j_1(\tau) + j_2(\tau)$. We first observe that the dynamics of j are similar to j_1 and j_2

$$\frac{\partial j}{\partial \tau} = \frac{\partial j_1}{\partial \tau} + \frac{\partial j_2}{\partial \tau} = \delta r j - q j.$$

And thus we can reduce the system to the system as we see it in equation 3.10. From this we found through time scale separation of the resource dynamics and the species dynamics that the quasi-steady state of the resource is given by

$$\bar{r}(\tau) = 1 - \frac{j_1(\tau) + j_2(\tau) + a(\tau)}{\rho} = 1 - \frac{j(\tau) + a(\tau)}{\rho},$$

after which we can solve the end of season state of j , a and b as shown in the previous sections (either including or excluding growing season death rate).

Now to retrieve the values of j_1 and j_2 observe that the ratio j_1/j_2 does not change during the growing season

$$\frac{\partial j_1/j_2}{\partial \tau} = \frac{j_2 j'_1 - j_1 j'_2}{j_2^2} = \frac{(\delta r - q) j_1 j_2 - (\delta r - q) j_1 j_2}{j_2^2} = 0.$$

Thus we can use the end of season value of j to get the end of season states of j_1 and j_2 by

$$\frac{j_i(\tau)}{j(\tau)} = \frac{j_i(0)}{j(0)} = \frac{j_i(1)}{j(1)} \quad \text{for } i = 1, 2.$$

Using the results of the previous sections we now give the year-to-year map from this years initial state to next years initial state of the system. This is found by applying the projection 4.25 to the end of season state of 4.24. We have $A_3 : \mathbb{R}^3 \rightarrow \mathbb{R}^3$ with

$$\begin{pmatrix} j_1 \\ j_2 \\ a \end{pmatrix} \mapsto \begin{pmatrix} \mu_d \beta(a) a + \mu_d a \ln \left(\frac{\beta(a)}{\beta(a) + \alpha(j_1 + j_2)(e^{\beta(a)} - 1)} \right) \\ \mu_d \frac{\beta(a) j_1 e^{\beta(a)}}{\beta(a) + \alpha(j_1 + j_2)(e^{\beta(a)} - 1)} \\ \mu_d a + \mu_d \theta \frac{\beta(a) j_2 e^{\beta(a)}}{\beta(a) + \alpha(j_1 + j_2)(e^{\beta(a)} - 1)} \end{pmatrix}. \quad (4.26)$$

4.3.1 Dynamics of the two year maturation model

To be able to judge the dynamics of the system we perform a numerical bifurcation analysis using *AUTO*. This shows how the trivial steady state loses stability through a transcritical bifurcation from which a non-trivial steady state appears. This in turn can go through a Neimark-Sacker bifurcation when a complex pair of eigenvalues crosses the unit circle. These dynamics are similar to the lower dimensional case. Figure 4.17 shows the bifurcation diagram of j_1 varying δ and θ . Also in figure 4.18 the limit cycle after the Neimark-Sacker bifurcation is visualised.

Since we now have a 3-dimensional map in contrast to the 2-dimensional map in the previous sections, we have an extra eigenvalue in addition to the complex conjugate pair of eigenvalues. It is possible for this eigenvalue to cross the unit-circle before the complex pair crosses the unit-circle. When this happens the system goes through a period doubling bifurcation and not through a Neimark-Sacker bifurcation. In this case we do not find an invariant curve. However, this appears to only happen when $\delta > 1$ which contradicts the assumptions of the model.

If the period doubling bifurcation happens after the Neimark-Sacker bifurcation it means the unstable steady state goes through a period doubling cascade. However, all the resulting orbits will be unstable and therefore do not appear through iteration of the map starting at a random initial value.

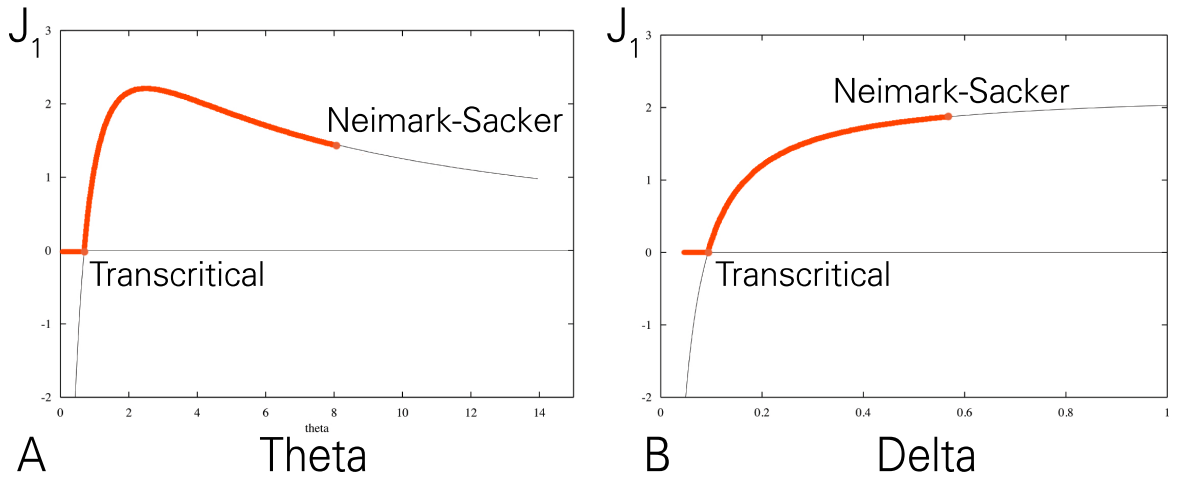


Figure 4.17: Two bifurcation diagrams of the map A_3 in (4.26), A varying θ and B varying δ . The red parts of the curves represent the stable solutions whereas the black parts represent the unstable solutions. The parameter values used were $\rho = 40, q = 0.01, \mu_d = 0.75$ and $\delta = 0.4$ for A and $\theta = 6$ for B.

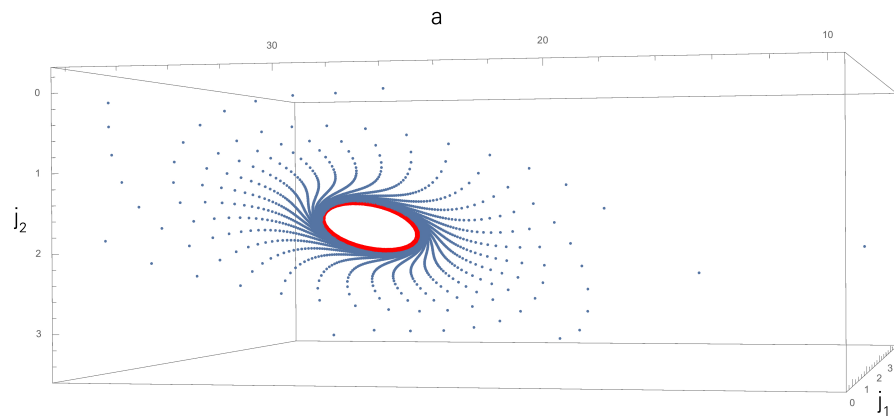


Figure 4.18: Positive semi-orbit of the point $(10, 2, 2)$ under iteration of the map A_3 in (4.26). We see this reveals an attracting limit cycle, which is visualised in red.

4.3.2 n -year maturation model

We can also extend this theory to a n -year maturation time. In this case the growing season dynamics can be solved in a similar fashion to the two year maturation case. We have the model

$$C_{n\text{-year maturation}} : \begin{cases} \frac{\partial r}{\partial \tau} = \rho r(1 - r) - r(j_1 + \dots + j_n) - ra, \\ \frac{\partial j_1}{\partial \tau} = \delta r j_1 - q j_1, \\ \vdots \\ \frac{\partial j_n}{\partial \tau} = \delta r j_n - q j_n, \\ \frac{\partial a}{\partial \tau} = 0, \\ \frac{\partial b}{\partial \tau} = \delta \theta r a - q \theta a, \end{cases} \quad (4.27)$$

in which we define $j(\tau) = j_1(\tau) + \dots + j_n(\tau)$. This reduces the system to (3.10), from which we can solve the end of season states. Applying the non-growing season projection gives the year-to-year map $A_{n+1} : \mathbb{R}^{n+1} \rightarrow \mathbb{R}^{n+1}$ with

$$\begin{pmatrix} j_1 \\ j_2 \\ \vdots \\ j_n \\ a \end{pmatrix} \mapsto \begin{pmatrix} \mu_d \beta(a) a + \mu_d a \ln \left(\frac{\beta(a)}{\beta(a) + \alpha(j_1 + \dots + j_n)(e^{\beta(a)} - 1)} \right) \\ \mu_d \frac{\beta(a) j_1 e^{\beta(a)}}{\beta(a) + \alpha(j_1 + \dots + j_n)(e^{\beta(a)} - 1)} \\ \vdots \\ \mu_d \frac{\beta(a) j_n e^{\beta(a)}}{\beta(a) + \alpha(j_1 + \dots + j_n)(e^{\beta(a)} - 1)} \\ \mu_d a + \mu_d \theta \frac{\beta(a) j_2 e^{\beta(a)}}{\beta(a) + \alpha(j_1 + \dots + j_n)(e^{\beta(a)} - 1)} \end{pmatrix}. \quad (4.28)$$

Through simulations of this model it is clear A_{n+1} is also able to give similar dynamics to that of the lower dimensional models. However, we have not further investigated the details of these since we have focussed on the smaller models.

4.4 Starvation

In the models so far we have assumed that throughout the growing season the value of $\delta r(\tau) - q$ remains positive, that is starvation does not occur. We have seen this is a valid assumption for a great range of parameter values.

However, at some point (when θ grows) the assumption is violated. At this point resource intake gets so large it creates starvation, and in the current models leads to negative values. To prevent this we can look at the model where birth potential and adult dynamics are split according to being in a growing phase or starvation

phase, following [20] & [13]. This leads to the growing season dynamics

$$C_2 \text{ year model : } \begin{cases} \frac{\partial r}{\partial \tau} = \rho r(1 - r) - rj - ra, \\ \frac{\partial j}{\partial \tau} = \delta rj - qj - \mu_c j, \\ \frac{\partial a}{\partial \tau} = \begin{cases} -\mu_c a & \delta r - q \geq 0 \\ \delta \theta r a - q \theta a - \mu_c a & \delta r - q < 0 \end{cases}, \\ \frac{\partial b}{\partial \tau} = \begin{cases} \delta \theta r a - q \theta a - \mu_c b & \delta r - q \geq 0 \\ \delta \theta r b - q \theta b - \mu_c b & \delta r - q < 0 \end{cases}. \end{cases} \quad (4.29)$$

This does not yield a nice analytic solution but is open to numerical investigation. From this we find the solutions become bounded to the first quadrant (all positive solutions). Also, when there is no starvation the resulting dynamics are clearly identical.

The general bifurcation scheme also stays similar with a stable trivial solution, a stable non-trivial solution and stable limit cycle. However, the system is able to return from a stable limit cycle to a stable non-trivial solution when θ or δ , indicating food intake, increases further. This signifies that at some point the food intake of the species grows so big such that the system cannot sustain the limit cycle behaviour anymore.

4.5 Chemostatic resource growth

The results so far only concern the models in which resource growth is governed by the logistic differential equation. We have also posed a model in which resource dynamics grows chemostatically, as for example in Sun [20]. Through time-scale separation we found a resource quasi-steady state of $\bar{r}(\tau) = \frac{\rho}{\rho + j(\tau) + a(\tau)}$ which does not produce a solvable system of equation for the slow dynamics. Therefore, we resort to a purely numerical investigation of this model.

We find we can reproduce similar behaviour to that of the logistic resource growth model by iteratively solving the system of equations numerically and applying the projection. Figure 4.19 shows how this can for example produce a stable spiral or attracting limit cycle similar to the results we have found earlier.

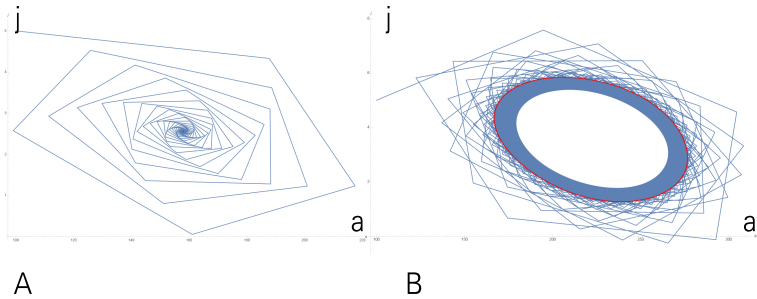


Figure 4.19: A and B show the positive semi-orbit of the point $(10,1)$ under iteration of the chemostatic model. For the parameter values in A we find a stable spiral towards an attracting non-trivial equilibrium point whereas in B an attracting limit cycle appears, both are visualised in red.

4.6 Niche Shift

We would also like to make the addition of a niche shift to the model, as is proposed in Sun [20]. In this case the adult population does not exclusively feed on a single resource but also feeds on a second resource whereas the juvenile population can only consume a single resource. The preference for either resource is modelled using a foraging preference η for resource 1 (on which the juvenile also feed) and $1 - \eta$ for resource 2 as is presented in figure 4.20.

The addition of a second resource r_2 means we also have two separate influx rates ρ_1 and ρ_2 belonging to the different resources respectively as well as two carrying capacities $R_{m,1}$ and $R_{m,2}$. The carrying capacities will be represented in the different values for δ_1 and δ_2 after rescaling with $\delta_1 = \sigma I_m R_{m,1}$ and $\delta_2 = \sigma I_m R_{m,2}$. In this we assume the intake rates and efficiencies for both resources are the same. This results in the continuous dynamics described by

$$C_{\text{two resource}} : \begin{cases} \frac{\partial r_1}{\partial t} = \rho_1 r_1(1 - r_1) - r_1 j - \eta r_1 a, \\ \frac{\partial r_2}{\partial t} = \rho_2 r_2(1 - r_2) - (1 - \eta)r_2 a, \\ \frac{\partial j}{\partial t} = \delta_1 r_1 j - qj, \\ \frac{\partial a}{\partial t} = 0, \\ \frac{\partial b}{\partial t} = \delta_1 \theta \eta r_1 a + \delta_2 \theta (1 - \eta) r_2 a - q \theta a. \end{cases} \quad (4.30)$$

The system in 4.30 can be analysed in a similar way we did previously using a time scale separation to derive a quasi-steady state for the resources r_1 and r_2 , after which the end of growing season states can be solved for through the same solution scheme as in the single resource case. This gives the end of growing-season

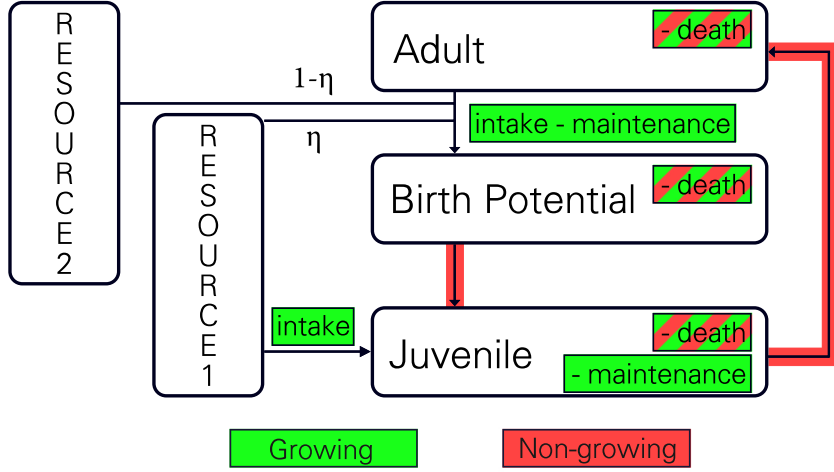


Figure 4.20: Outline of the relations between the different variables in the system with two resources.

juvenile state

$$j(1) = \frac{\beta_\eta(a_0) j_0 e^{\beta_\eta(a_0)}}{\alpha j_0 e^{\beta_\eta(a_0)} + \beta_\eta(a_0) - \alpha j_0},$$

with a slightly different $\beta_\eta(a_0) = \delta_1 - q - \frac{\delta_1 \eta}{\rho_1} a_0$ and $\alpha = \frac{\delta_1}{\rho_1}$. As well as the end of growing-season birth potential

$$b(1) = \theta \left(\eta \delta_1 + (1 - \eta) \delta_2 - q - \left(\frac{\delta_1 \eta^2}{\rho_1} + \frac{\delta_2 (1 - \eta)^2}{\rho_2} \right) a_0 + \theta \eta a_0 \ln \left(\frac{\beta_\eta(a_0)}{\beta_\eta(a_0) + \alpha j_0 (e^{\beta_\eta(a_0)} - 1)} \right) \right).$$

We use these end of season states and a projection as in (3.11) to derive a two-dimensional map from the current initial values to next years initial values for the growing season. The map then becomes $A_\eta : \mathbb{R}^2 \rightarrow \mathbb{R}^2$ with

$$\begin{pmatrix} j_n \\ a_n \end{pmatrix} \mapsto \begin{pmatrix} \mu_d \left(\eta \delta_1 + (1 - \eta) \delta_2 - q - \left(\frac{\delta_1 \eta^2}{\rho_1} + \frac{\delta_2 (1 - \eta)^2}{\rho_2} \right) a_n \right) a_n + \mu_d \eta a_n \ln \left(\frac{\beta_\eta(a_n)}{\beta_\eta(a_n) + \alpha j_n (e^{\beta_\eta(a_n)} - 1)} \right) \\ \mu_d a_n + \mu_d \theta \frac{\beta_\eta(a_n) j_n e^{\beta_\eta(a_n)}}{\beta_\eta(a_n) + \alpha j_n (e^{\beta_\eta(a_n)} - 1)} \end{pmatrix}, \quad (4.31)$$

We note that for $\eta = 1$ this is identical to the map in (4.7).

When we look at the bifurcation diagram for various values of η we find the bifurcation scheme is not changed from the one we had in a single resource model, where the system goes through a transcritical bifurcation and a Neimark-Sacker bifurcation. Even for the value $\eta = 0$ where the species feed on completely different resources this remains intact. In figure 4.21 we provide a numerical two parameter

analysis of the Neimark-Sacker bifurcation for different values of η and θ . This illustrates how the bifurcation point varies for different foraging preferences. From which we can conclude that not only competition for the same resource but also delayed feedback is a cause for the population cycles that can be observed.

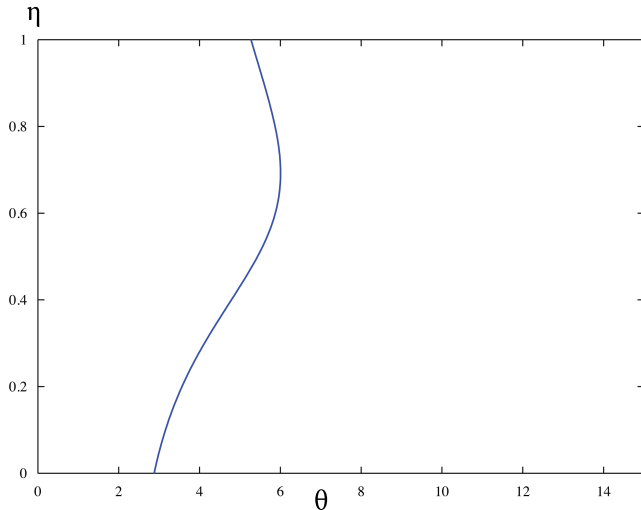


Figure 4.21: Two parameter bifurcation diagram for the Neimark-Sacker bifurcation of the map A_η in 4.31. The non-trivial steady state becomes unstable through a Neimark-Sacker bifurcation when moving from the left plane to the right plane.

5 Conclusion

In this thesis we develop a modelling technique which includes seasonality in a population model through the semi-discrete modelling of a growing and a non-growing season. The resource-consumer interaction studied includes a stage-structure in the consumer population that distinguishes between a juvenile (not reproducing) and adult (reproducing) population. Reproduction is governed by a birth potential that increases during the growing season and is released as a discrete event during the non-growing season, which is a reasonable assumption for many yearly reproducing animals.

The consumer species is assumed to be iteroparous. This is in contrast to the model considered by for example Geritz & Kisdi [18] or Davydova, Diekmann & van Gils [22], which consider semelparous species only reproducing a single time. Therefore, the model considered here is better applicable to larger mammals which are generally iteroparous.

The maturation of the juveniles is considered to be a yearly event where in first instance we consider a precocious species for whom maturation happens after a single year. This model is extended to a model in which maturation is more delayed and takes multiple years. The former is more likely when considering small mammals or birds, the latter would be better suited to the modelling of larger mammals.

The maturation of individuals at a certain age is a clear difference with models where maturation is resource dependent and happens after reaching a certain threshold body size [20]. This simplification of the model is a necessary assumption to be able to derive the discrete year to year map we study. It can be discussed whether this is a valid assumption which might be more reasonable for certain species than for others.

Applicability of the model is largely based on the timing of giving birth and mating and the length of the gestation period. When mating occurs early in the growing season and animals have a long gestation period the accumulation of birth potential during the growing season seems reasonable. Even when this is not the case but when feeding during the growing season leads to larger birth size for the following season the assumption can be applicable. This also makes the assumption of discrete maturation more sensible. Therefore, the model presented seems more suitable for larger mammals such as deer, bears or possibly larger fish species. Whereas for animals with short gestation periods the whole concept of modelling

using a birth potential that accumulates during the entire growing season seems questionable.

By solving the growing-season dynamics when the resource is considered to reach a fast quasi-equilibrium we were, in the case of logistic resource growth, able to derive a discrete map giving the yearly dynamics of the consumer. From this we derived a domain for a non-trivial steady state and proved existence under the condition of the trivial steady state being unstable. Furthermore, we numerically showed how this non-trivial steady state can lose stability through a Neimark-Sacker bifurcation which produces either a dense solution on an invariant curve or periodic solutions.

The finding of periodic behaviour shows the models can be used as an explanation for the behaviour of larger mammal species or birds in which population cycles appear. Cycles in population levels can be observed in many species [25],[26] and many explanations can be found including predation and periodic environments however we provide an explanation which does not need these mechanisms.

Neubert & Caswell [27] have already shown how density dependence in growth and juvenile survival can produce population cycles through a Neimark-Sacker bifurcation. However, these models do not have a mechanistic interpretation coming from the interactions of the different species in the model. The addition of a continuous growing season that models the resource-consumer interaction does provide such an interpretation.

We also considered the extension of the consumer going through a niche shift when maturing such as is considered by Sun [20]. We show how this does not qualitatively change the dynamics of the discrete map for the yearly consumer values. We also numerically investigate whether including the possibility of starvation or chemostatic resource growth changes the dynamics but find no qualitative differences.

It would be interesting to consider adding higher trophic levels to the model to be able to include the effect of predation of the consumer species. As well as considering the extension of a male and female population in which the females are the ones generating the birth potential since in the current model the complete population generates birth potential.

Bibliography

- [1] Ricker, W.E., *Stock and recruitment*, J. Fish. Res. Bd. Canada, **11**, 559-623, 1954.
- [2] Beverton, R.J.H. & Holt, S.J., *On the dynamics of exploited fish populations*, Fisheries investigations, series 2, **vol 19**, London, UK: Her Majestys Stationery Office, 1957.
- [3] Nicholson, A. J. & Bailey, V. A., *The Balance of Animal Populations.-Part I*, Proceedings of the Zoological Society of London, **105**, 551-598, 1935.
- [4] Murdoch, W., Briggs, C. & Nisbet, R., *Consumer-Resource Dynamics (MPB-36)*, Princeton University Press, 2003.
- [5] Bernardelli, H., *Population waves*, J. Burma Res. Soc. **31**, 1-18, 1941.
- [6] Lewis, E.G., *On the generation and growth of a population*, Sankhya: The Indian Journal of Statistics **6**, 93-96, 1942.
- [7] Leslie, P.H., *On the use of matrices in certain population mathematics*, Biometrika **33**, 183-212, 1945.
- [8] Caswell, H., Trevisan, M.C., *Sensitivity analysis of periodic matrix models*, Ecology **75**, 1299-1303, 1994.
- [9] Katsanevakis, S., Verriopoulos, G., *Seasonal population dynamics of octopus vulgaris in the eastern mediterranean*, ICES J. Mar. Sci. **63**, 151-160, 2006.
- [10] McFadden, C.S., *A comparative demographic analysis of clonal reproduction in a temperate soft coral*, Ecology **72**, 1849-1866, 1991.
- [11] De Roos, A. M., Diekmann, O. & Metz, J. A. J., *Studying the dynamics of structured population models: a versatile technique and its application to Daphnia*, Am. Nat. **139**, 123-147, 1992.
- [12] De Roos, A.M., Schellekens, T., van Kooten, T., et al., *Food-dependent growth leads to overcompensation in stage-specific biomass when mortality increases: the influence of maturation versus reproduction regulation.*, Am. Nat. **170**, E59-76, 2007.

- [13] De Roos, A.M., Schellekens, T., van Kooten, T., et al., *Simplifying a physiologically structured population model to a stage-structured biomass model.*, Theor. Popul. Biol. **73**, 47-62, 2008.
- [14] Guill, C., *Alternative dynamical states in stage-structured consumer populations.*, Theor. Popul. Biol. **76**, 168-178, 2009.
- [15] Wollrab, S., De Roos, A.M., Diehl, S., *Ontogenetic diet shifts promote predator-mediated coexistence.*, Ecology **94**, 2886-2897 2013.
- [16] Gyllenberg, M., Hanski, I. & Lindstrom, *Continuous versus discrete single species population models with adjustable reproductive strategies.*, B. Math. Biol. **59**, 679-705, 1997.
- [17] Gamarra J. G. P. & Sole R. V. , *Complex Discrete Dynamics from Simple Continuous Population Models.*, Bulletin of Mathematical Biology **64**, 611-620, 2013.
- [18] Geritz, S.A.H., Kisdi, E., *On the mechanistic underpinning of discrete-time population models with complex dynamics.*, J. Theor. Biol. **228**, 261-269,, 2004.
- [19] Eskola H.T.M., Parvinen K., *On the mechanistic underpinning of discrete-time population models with Allee effect*, Theoretical Population Biology **72**, 41-51, 2007.
- [20] Sun, Z., De Roos, A.M., *Alternative stable states in a stage-structured consumer-resource biomass model with niche shift and seasonal reproduction*, Theoretical Population Biology **103**, 60-70, 2015.
- [21] Utz, M., Kisdi, E., Doebeli, M., *Quasi-Local Competition in Stage-Structured Metapopulations: A New Mechanism of Pattern Formation*, Bulletin of Mathematical Biology **69**, 1649-1672, 2006.
- [22] Davydova, N.V., Dieckmann, O., Van Gils, S.A., *Year class coexistence or competitive exclusion for strict biennials?*, J. Math. Biol. **46**, 95-131, 2003.
- [23] Arnold, V.I. *Geometrical Methods in the Theory of Ordinary Differential Equations*, Springer-Verlag New York, 1983.
- [24] Kuznetsov, Y., *Elements of Applied Bifurcation Theory*, Springer-Verlag New York, 1998.
- [25] Bulmer, M.G., *A statistical analysis of the 10-year cycle in Canada*, Journal of Animal Ecology, **43**, 701-718, 1974.

- [26] Watson, A., Moss, R., Rothery, P., Parr, R., *Demographic causes and predictive models of population fluctuations in Red Grouse*, Journal of Animal Ecology, **53**, 639-662, 1984.
- [27] Neubert, M and Caswell, H, *Density-dependent vital rates and their population dynamic consequences*, J. Math. Biol., **41**, 103-121, 2000.